[Frontiers in Bioscience 13, 1535-1556, January 1, 2008]

Molecular imaging as the main part of our decision-making and treatment strategies in stroke

Amir Kashefi[1], Heng Zhao[2], Xiaoyuan Chen[1]

[1] Department of Radiology Molecular Imaging Program at Stanford (MIPS) and Bio-X Program, Stanford University School of Medicine, CA, [2] Department of Neurosurgery, Stanford Stroke Center, Stanford, CA

TABLE OF CONTENTS

1. ABSTRACT

Review of results of clinical studies indicates the number of potential patients who are actually treated for acute ischemic stroke is disappointingly low, and effective treatments are making a minor impact on this major public health problem. Imaging modalities, such as diffusion- and perfusion-weighted images, as well as CT perfusion and CT angiography, to better select patients for treatment are now routinely performed in most academic medical centers. However, there is not a perfect penumbra imaging technique and each one has its own advantages and disadvantages. Recent advances in molecular imaging modalities allow a better understanding of this pathophysiological process that could lead to enhanced therapy for stroke. This article seeks to describe the role of molecular imaging in identifying the pathophysiology of stroke and how it could be incorporated in future decision-making and treatment strategies in stroke.

2. MOLECULAR IMAGING

Molecular imaging has emerged as a potentially revolutionary discipline that aims to visually characterize normal and pathologic processes at the cellular and molecular levels within the milieu of living organisms. It broadly incorporates methods and concepts from molecular and cell biology, imaging sciences, chemistry, high-throughput biology (e.g., genomics, proteomics), nanotechnology, pharmacology, and bioinformatics (1-3). And through molecular imaging, radiology is expected to play a critical role in advancing molecular medicine and potentially revolutionizing patient care and biomedical research (4, 5).

Conventional clinical imaging generally relies on macroscopic anatomic and physiologic variations for disease diagnosis and assessment. Such morphologic changes are often nonspecific and late phenotypic

Table 1. Attributes of molecular imaging modalities

Modality	Sensitivity	Spatial resolution	Temporal resolution	Penetration Depth
SPECT	Medium	Low	Low	High
PET	High	Low	Low	High
MRI	Low	High	High	High
US	Medium	Medium	High	Medium
Optical Imaging	High	Low	High	Low

Adapted with permission from reference 1.

manifestations of underlying molecular derangements (1, 6). By contrast, molecular imaging exploits the use of directed imaging probes to sense the specific molecular alterations underlying diseases rather than downstream end effects at the tissue or organ level which means earlier and more precise disease diagnosis, improved disease characterization, and more meaningful monitoring of disease progression.

The impact of molecular imaging in biomedical research is also promising. *In vitro* research traditionally extracts and studies the events in artificial environments like cell cultures. This is problematic because biologic processes rarely occur in isolation and are instead mediated through a complex and dynamic interplay of gene expression, signaling pathways, environmental factors, and inherent feedback mechanisms. In contrast, biology can be studied under physiological conditions within the intact microenvironment and without any tissue destruction by the application of molecular imaging. This transition from a reductionism to a holistic approach to research (7) enables molecular imaging to be more predictive and relevant in research studies. Molecular imaging also enables real-time monitoring of molecular phenomena through repetitive imaging of an individual subject. Molecular imaging has been rapidly adopted into the basic science research of dynamic biologic processes such as hypoxia (8), inflammation (9), apoptosis (10), angiogenesis (11), tumorigenesis (12), and gene expression (13, 14). More translational applications include stem cell trafficking (15) and monitoring of the distribution and efficacy of novel therapeutic moieties (16). In fact, one of the most promising applications of molecular imaging is to accelerate drug discovery and development.

Imaging modalities used in molecular imaging include positron emission tomography (PET), single photon emission computed tomography (SPECT), magnetic resonance (MR) imaging, optical imaging, and ultrasound (US). These modalities differ in terms of spatial resolution, temporal resolution, sensitivity in probe detection, depth of signal penetration, availability of biocompatible molecular imaging agents, and, of course, cost. Each has its unique advantages and disadvantages, and the choice of imaging system ultimately depends on the question to be addressed (Table 1). These modalities in combination with contrast agents, which are a broad set of molecular probes and tracers that target a specific peptide, receptor ligand, enzyme substrate, oligonucleotide, or antibody, are the basis of molecular imaging technology.

A survey of the molecular imaging literature reveals that its application to human ailments is being explored in a range of disparate fields from neurology and psychiatry to infectious diseases and drug resistance. The goals of this review are to provide a summary of molecular imaging application in stroke and to stimulate discussion among scientists about whether and how it could be incorporated in future decision-making and treatment strategies in stroke.

3. STROKE

Stroke is the leading cause of disability and the third leading cause of death in the USA. Approximately 700,000 strokes occur in the united states annually (17, 18). The clinical burden of stroke and transient ischemic attack now exceeds that of coronary heart disease (19). The American Heart Association (AHA) estimates the cost of treating stroke related injury and disability at $58 billion for 2006 alone (www.americanheart.org).

Treatment of stroke requires a comprehensive understanding of stroke pathophysiology. In ischemic stroke, which represents about 80% of all strokes, decreased or absent circulating blood deprives neurons of necessary substrates. A thrombus or an embolus can occlude a cerebral artery and cause ischemia in the affected vascular territory. The obvious therapeutic response to such a reduction of blood supply is to re-establish flow by pharmacologic or mechanical means as quickly as possible, leading to the advent of the only FDA approved and available therapy for stroke, which is the intravenous (IV) tissue plasminogen activator (tPA) within 3 hours of stroke onset. This treatment is only effective within 3 hours of onset and only treats the symptoms by dissolving the clot. Only 2-3% of stroke patients are able to use this agent because of its narrow therapeutic window. It also has a limited success rate of 35–65% at recanalizing the middle cerebral artery, dropping to about 10% if the internal carotid artery is occluded (20, 21). The disappointing result has been that intravenous tPA for the treatment of stroke has made only a minor impact on a major public health problem. Combined analysis of the tPA clinical trials has demonstrated that the earlier initiation of tPA therapy is associated with improved outcomes which is directly related to the concept of the ischemic penumbra and its evolution (22).

The concept of the ischemic penumbra is familiar to most investigators who work in the stroke field. In brief, the initial definition of the ischemic penumbra by Astrup *et al* (23), was that portion of the ischemic zone with absent electrical activity but with preserved ion homeostasis and transmembrane electrical potentials. Several revised definitions of the ischemic penumbra appeared over time that focused on thresholds of cerebral blood flow (CBF) decline, energy metabolism and protein synthesis. From the

clinical perspective, a relatively simple and straightforward definition of the ischemic penumbra initially proposed by Hakim (24) is that portion of the ischemic region destined for infarction that is currently potentially salvageable with appropriate intervention. This definition provides a framework for approaching the important concepts of evolution of penumbra into infarcted tissue, the time window over which this evolution occurs (i.e. the therapeutic time window) and the use of imaging modalities to identify at least an approximation of this vital ischemic region.

4. NEUROIMAGING AND STROKE

Brain imaging plays a vital role in acute stroke by delineating ischemia from hemorrhage, estimating tissue at risk for infarction and excluding some stroke mimics, such as tumor. Neuroimaging modalities have emerged as integral components of almost all acute stroke trials, which may be used for diagnostic, therapeutic, and prognostic purposes in acute stroke and beyond.

The mainstays of early stroke diagnosis are conventional noncontrast head CT (NCCT) and conventional brain MR imaging (25-33). Emergency, non-contrast CT of the head is the recommended initial neuroimaging study (34). This modality identifies hemorrhage and can help distinguish non-vascular causes of neurological symptoms such as tumor (35). CT is not ideal, however, because of the difficulty in detecting acute or small infarcts and artifact in the brainstem area (34).

In some centers, multiparametric MRI is increasingly used as first-line imaging for patients with suspected ischemic stroke. MRI is better for detection of acute ischemia than CT (36). Diffusion-weighted imaging (DWI) sequences should be done in all acute MRI studies to allow identification of ischemic areas within minutes of symptom onset (37, 38). DWI reveals areas of restricted Brownian motion of water molecules likely due to cytotoxic edema. The sensitivity and specificity of DWI for detecting acute ischemia are about 100%. Diffusion-weighted imaging also provides the additional advantage of visualization of small subcortical lesions and brainstem or cerebellar lesions, usually poorly visualized on CT (39-46). The diagnosis of ischemia may be confirmed by finding corresponding hypointense lesions in a vascular distribution on apparent diffusion coefficient (ADC) maps.

As complementary sequences in a dedicated stroke protocol MRI, magnetic resonance angiography (MRA) and perfusion-weighted imaging (PWI) may provide additional information regarding vessel status, collateral flow, and territories at risk. MRA allows for rapid characterization of the cervical and cephalic large vessels. MRA may delineate extracranial internal carotid artery stenosis with high accuracy compared with digital subtraction angiography (DSA) (47-49).

Dynamic CT perfusion imaging and CT angiography (CTA) have shown remarkable progress in providing information in acute stroke. Dynamic CT perfusion is acquired using sequential imaging in cine mode after intravenous injection of an iodinated contrast medium (50). The data are then processed using either a maximal-slope model or a deconvolution analysis to produce maps of cerebral blood flow (CBF), cerebral blood volume (CBV), time to peak (TTP), and mean transit time (MTT). Dynamic CT perfusion imaging showed good correlation with MRI for CBF and MTT abnormalities in acute stroke (51) and several studies have suggested that CT has the potential of replacing MRI. Nonetheless, DWI remains the sole imaging technique within minutes of onset regardless of location and size, and it is still unlikely to be replaced by CT in the foreseeable future ((52). CTA has been demonstrated to be accurate in the evaluation of cervical and large-vessel intracranial occlusion.

Carotid Duplex ultrasound (CDUS) and transcranial Doppler (TCD) ultrasound are noninvasive methods for neurovascular evaluation of the extracranial and intracranial large vessels. Although both methods may help to establish the source of an embolic stroke, they have rarely been used acutely for this purpose. However, accumulating evidence suggests that both Duplex and TCD can be used urgently at the bedside to select patients for interventional thrombolytic or endovascular treatment (53-56).

The penumbra is the target tissue for early thrombolysis and can be visualized by various imaging modalities, including PET, CT and MRI (57-60). PET provides quantitative measurements of CBF, CBV, the metabolic rate of oxygen consumption ($CMRO_2$), and the rate of oxygen extraction (OEF). In PET studies, the penumbra is characterized by the pattern of increased OEF with reduced CBF and $CMRO_2$ identifies penumbral tissue (61). Moreover the PET ligand ^{18}F-fluoromisonidazole (^{18}F-FMISO) is a marker of hypoxic but still viable tissue. Studies with this presumed penumbral marker have confirmed the prolonged existence of penumbral tissue in stroke models and patients (62). In MRI studies, the equivalent of the penumbra is called “mismatch”, which can be visualized by a combination of DWI and PWI (63). Minutes after the onset of stroke, MR DWI can demonstrate restriction of the random motion of water and decline of its ADC (64). This is being used as a marker of irreversible neuronal damage resulting from critically severe tissue hypoperfusion. Moreover, identifying a mismatch between such a diffusion lesion and the extent of the perfusion abnormality on PWI has in turn evolved as a means of depicting the potentially viable penumbra. The CBF/CBV mismatch on perfusion CT correlates well with regions of DWI/PWI mismatch when both studies are obtained in a close temporal window (65). The validation of the thresholds required to identify the abnormal CBF and CBV regions remains to be proven. Other problems with perfusion CT include the need to inject iodinated contrast to obtain the images and the relatively restricted tissue volume that can be imaged currently. DWI/PWI MRI can essentially image the whole brain and is not restricted to several slices as perfusion CT currently is. Another problem with perfusion CT as compared to DWI/PWI is the tracking of presumed infarct volumes over time.

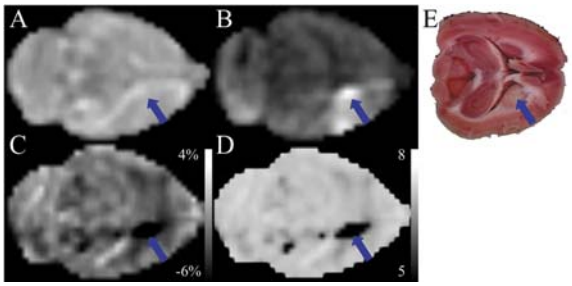

Figure 1. Comparison of horizontal T_2-weighted image (A), isotropic diffusion-weighted image (B), absolute magnetization transfer ratio asymmetry image (C), absolute pH image (D), and 2,3,5-TTC-stained histology (E) of an ischemic rat brain. The ischemic area (arrow) is located in the caudate nucleus, a region that commonly becomes affected after occlusion of the MCA. No effect of ischemia was visible on the T_2-weighted image (A), but the pH-sensitive images (C and D) show the ischemic region, as confirmed by the diffusion-weighted image (B), and by histology, which was acquired 8 h later (E). Adapted with permission from ref. 72.

Although currently diffusion and perfusion MRI is widely used in clinical trials to approximate the location and persistence of the ischemic penumbra, to select appropriate patients for inclusion and to evaluate the treatment effect (52), recent evidences which have route in molecular imaging are questioning many of its principal assumptions.

Lin *et al.* (66) explored the relationship between CBF and ADC and showed that after an initial gradual decline, an abrupt and significant reduction of ADC occurs at CBF values around 15 mL/100 g/min. However, the threshold was time dependent, rising to 24 mL/100 g/min at later time points. Beyond method-related errors, this time dependence may explain why some studies have reported ADC changes at CBF as high as 50 mL/100 g/min and explain the difficulty of identifying an absolute ADC threshold for irreversible damage (67). On the other hand, Nicoli *et al.* (68) using MR spectroscopic imaging demonstrated that within regions of severe ADC decrease, a heterogeneous pattern of metabolic injury exists, evidenced by wide variations in lactate and N-acetyl aspartate ratios. Also, in a recent study using multitracer PET, Guadagno *et al.* (69) documented that the DWI lesion does not represent a single stage of the ischemic process and that it incorporates potentially salvageable penumbral tissue. They demonstrated a heterogeneous pattern of blood flow, oxygen metabolism, and extraction fraction within the DWI lesion, inconsistent with the notion of uniformly irreversible neuronal damage. Furthermore, in a subsequent report, they showed that severe ADC reduction existed in the penumbra as well as the core (70), and thus cannot solely represent irreversible damage. Loh *et al.* (71) have also found areas of reduced ADC outside of the acute DWI lesion that did not progress to infarction and thus argue against an absolute threshold based on ADC alone.

Recently, Zhou *et al.* (72) developed a new MRI approach based on a magnetization transfer (MT) experiment in which the exchangeable amide protons of mobile tissue proteins and peptides are selectively irradiated using radiofrequency. This causes saturation of these protons, which is subsequently transferred to the water protons. Even though the concentration of such cellular proteins and peptides is in the micro- to millimolar range, these effects can be detected as a few percent signal change in the water line through a sensitivity enhancement mechanism. Sun *et al.* (73) used this technique to acquire pH-weighted images during acute ischemia and showed that the outer boundary of the hypoperfused area that shows a decrease in pH without DWI abnormality may better correspond to the classic ischemic penumbra border than the PWI deficit (Figures 1 and 2).

In a recent pilot study, Blankenberg *et al.* using ^{99m}Tc-HYNIC-annexin V SPECT imaging in acute stroke showed that human image data of that annexin V uptake correlates to sites of restricted diffusion on MRI. The regions of restricted diffusion seen on MRI also appeared to be more uniform than the heterogeneous multifocal uptake of annexin V. This may imply that annexin V imaging better reflects sites of varying degrees of brain injury as compared with DWI MR imaging on a molecular level (74). Thus, the current uncertainties surrounding MR diffusion-perfusion imaging indicate that the "mismatch" does not always "match" the penumbra (58, 66-71, 73-75). The key question is "how important is the molecular imaging role in penumbra imaging and stroke treatment?"

4.1. Molecular imaging of the penumbra

A better identification of the true penumbral tissue might rely on the cascade of molecular events started after vascular occlusion that have been the objective of extensive research in recent years and development of new strategies for stroke treatment hinges on better understanding of this complex cellular and molecular interplay that ensue following stroke. Thus, penumbra as the primary target of acute stroke therapy suggested that imaging identification of the penumbra could be of great value in the selection of patients for acute stroke therapy.

4.1.1. Molecular imaging of hypoxia

Recently, ^{18}F-FMISO PET imaging of stroke patients has been investigated as a possible penumbral imaging method, which, because of the direct imaging of cellular hypoxia, may overcome some of the difficulties with existing indirect perfusion-based imaging methods. Nitroimidazole compounds such as ^{18}F-FMISO diffuse freely across cell membranes and in living cells are then reduced by intracellular reductases into a radical anion. In normoxic conditions, this compound is rapidly reoxidized and diffuses back out of cells. Under hypoxic conditions, that is, inadequate oxygen supply relative to demand, however, further reduction steps occur, and the reduced compound becomes irreversibly bound to intracellular macromolecules. Thus, reduced nitroimidazoles are supposed to be trapped within hypoxic cells, but not by necrotic or nonhypoxic cells (76).

Human ^{18}F-FMISO studies have been revealing about the temporal and spatial evolution of hypoxia in

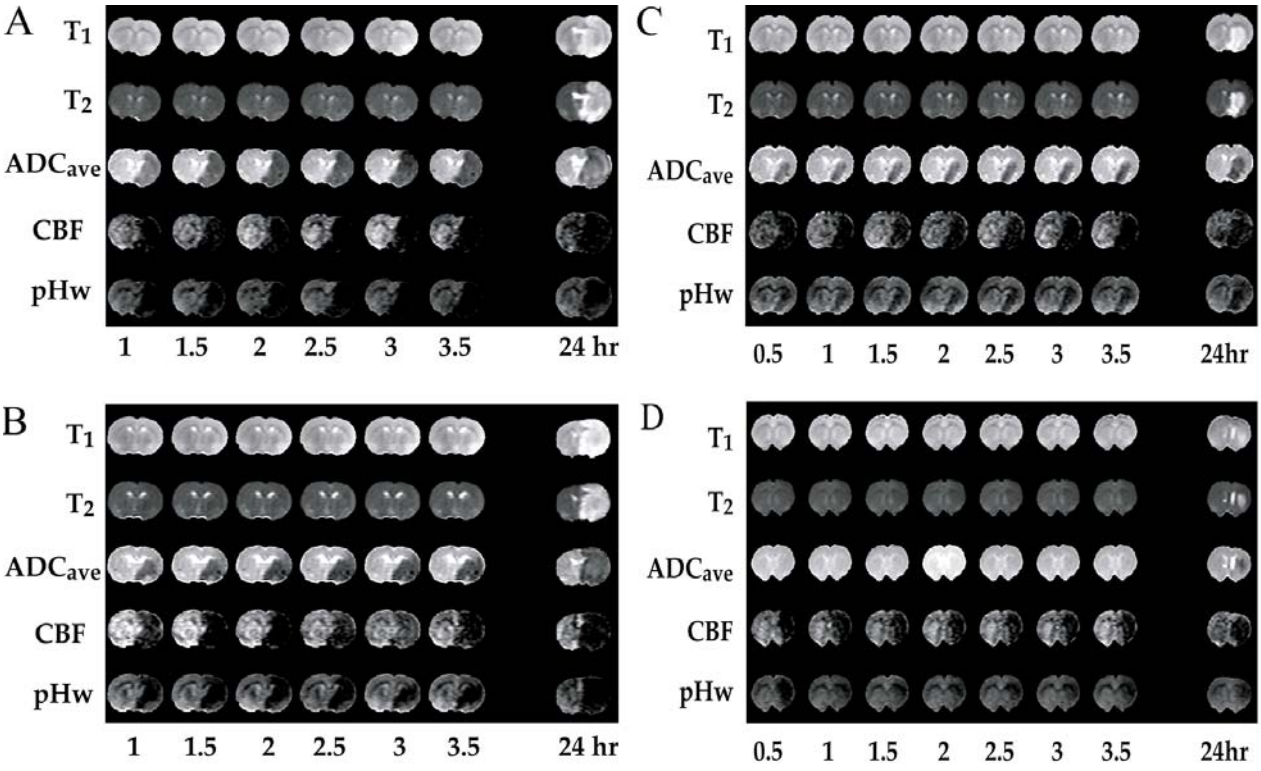

Figure 2. Example images of ischemic animals in Groups I–II. (**A**) Group I: classic PWI/DWI match (within 20%) throughout acute period, confirmed by corresponding T_2 lesion at 24 h. (B–D) Group II: classic PWI/DWI mismatch (>20%). In (B), a heterogeneous pHWI deficit at 0.5 to 1 h evolves to match (within 20%) the hypoperfusion region within 3.5 h. The ADC_{ave} deficit evolves slower, but at 24 h all image methods match the final T_2-deficit. In (C), pHWI abnormality is smaller than the PWI deficit and grows only slightly. The ADC_{ave} deficit is within the pHWI lesion and also does not evolve much. At 24 h, infarction area in T_2 visually corresponds to the 3.5 h pHWI deficit. In (D), there is no ADC_{ave} deficit within the first 3.5 h. At 24 h, there is an infarct, as expected based on the presence of a pHWI deficit at 3.5 h. Adapted with permission from ref. 73.

stroke and in correlating these changes with clinical outcome. However, there are some unresolved questions that are not easily answered in human studies. As, is binding specific to hypoxic tissue, or will there be ongoing binding after reperfusion (either spontaneous or after thrombolytic therapy)?

Takasawa *et al.* (77) in a recent pilot study in rats, showed that trapping of ^{18}F-FMISO in the stroke area only occurred in the early phase of middle cerebral artery occlusion (MCAO), but not when tissue necrosis has developed (i.e. 48 h after permanent MCAO) or if early reperfusion has occurred, which strongly support the validity of ^{18}F-FMISO as a specific marker of the viable hypoxic brain/penumbra after stroke (Figure 3).

4.1.2. Molecular imaging and energy metabolites

The concentration of energy metabolites including ATP, phosphocreatine, lactate and *n* -acetyl aspartate (NAA), differs between the ischemic core and the penumbral tissue where the metabolite concentration decrease is less severe (78) so the use of a molecular imaging technique might be helpful to characterize the ischemic penumbra in individual patients.

MR spectroscopy (MRS) has been used *in vivo* to estimate the concentration of certain metabolites such as creatine, choline, NAA, lactate, myoinositol, glutamate/glutamine, and lipids (79). The physical basis of MRS is the chemical shift effect, that is, the fact that nuclei located in different molecular environments (different molecules or different locations within a molecule) sense slightly different magnitudes of magnetic field, causing them to precess at different rates.

MRS provides plots (spectra) of signal intensity, which is proportional to concentration, versus precession rate shift with respect to a reference, expressed in parts per million (ppm). Even though any nucleus with nonzero spin could in principle be studied, clinical MRS practice is most commonly based on the hydrogen nucleus. Molecular groups generate specific resonance patterns on the spectrum, either as single peaks, doublets, or more complex shapes. A given molecule therefore may have multiple corresponding peaks, only some of which may be observable. As magnetic field strength is increased, the separation of peaks improves, increasing the number of metabolites that can be distinguished. Especially at low field strengths, observed peaks may contain contributions

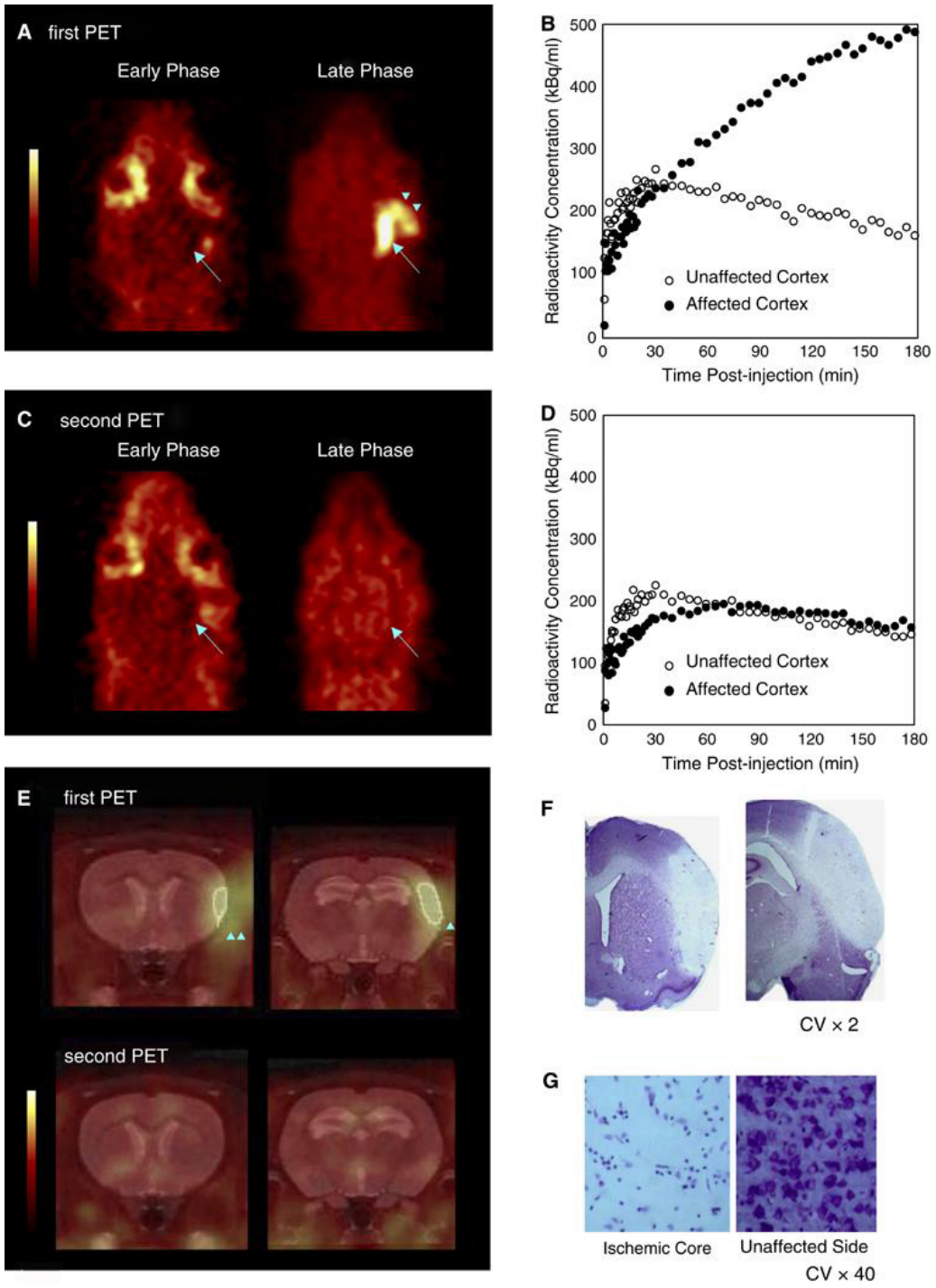

Figure 3. Positron emission tomography data and histology in the permanent MCAo rat . (A) Early phase (sum of first 10 frames, that is, 0 to 5 mins) and late phase (sum of last 10 frames, that is, 130 to 180 mins) for the first PET session (started 39 mins after clip on), showing prominent late trapping of the tracer in the affected cortex (arrow), and some trapping as well in the surgically injured temporalis muscle (arrowheads); (B) Time–activity curves (TACs) for the affected and unaffected sides for the first PET session. (C) Early phase and late phase accumulated images for the second PET session (48 h later; same frames as first session), showing symmetrical late retention; (D) TACs for the affected and unaffected sides for the second PET session. (E) Fusion images with MRI template (coronal images), also illustrating the affected cortex ROI on two slices (see Materials and Methods), and the surgically injured temporalis muscle (arrowheads); (F) illustrative Cresyl Violet (CV) coronal sections at approximately the same levels as in (E); (G) CV at high magnification. Adapted with permission from ref. 77.

from several affine molecular types and locations. MRS studies can be carried out for a single voxel or for a matrix of voxels. Due to a number of confounding measurement variables, reliable quantification is very difficult to achieve; therefore, concentrations are usually expressed in arbitrary units, or as ratios. As the chemical shift in ppm is constant for all peaks, prior knowledge can be used for their identification and fitting.

A parameter known as echo time (TE) controls the delay from the radiofrequency excitation pulse to the detection of the echo. Due to different T2 relaxation times among metabolites, changing the TE changes the appearance of the spectrum. Short echo times (on the order of 20-40 ms) result in spectra containing contributions from a large set of metabolites and macromolecules, which may be difficult to separate; long echo times (on the order of 120-300 ms) result in spectra with a flatter baseline, on which only creatine, choline, NAA, lactate, and lipids are visible (80).

Detection of lactate by *in vivo* proton MRS may provide useful information on metabolic stress in brain, potentially identifying the degree of ischemia (81-84). Therefore, if lactate can be quantitatively evaluated, it could have an important clinical impact. However, a large part of the lactate signal overlapped with lipid signals in conventional MRS measurements (85, 86). Thus, lactate has been thought to rise early after the insult in the acute phase (<24 h) and may remain high over a long period into the chronic phase (>7 days) (87), which could lead us to an inappropriate understanding of the pathophysiological status in the ischemic lesion.

Harada *et al.* (88) in a recent study using 7 Tesla MRS and stimulated echo acquisition mode (STEAM) with longer TE demonstrated that MRS-detectable lactate increased rapidly in the infarcted rat brain 6 h after MCAO and disappeared within 48 h following MCAO. In addition, MRS detectable lipid was also observed 6 h after MCAO and continued increasing over 1 week, which was confirmed by histological examination.

Thus, MRS at higher field strengths provides better signal to noise ratio (SNR) and increased spectral, spatial and temporal resolution, allowing the acquisition of high quality, easily quantifiable spectra in acceptable scan times (88). This may provide precise biochemical information from distinct regions of the brain noninvasively that is clinically useful by evaluating the severity of cerebral ischemia and the status of the patient in response to the therapy.

Moffet *et al.* (89) have recently summarized evidence from numerous studies showing that reduced NAA levels as detected by MRS can be an extremely valuable marker of brain injury after stroke or hypoxia. *In vivo* MRS studies support the hypothesis of NAA as a surrogate for neuronal loss and dysfunction, and the clinically associated neurological deficits observed in patients after local or global hypoxia-ischemic incidents. However, several key issues including the basis of the relatively slow observed decreases in NAA signal after the onset of stroke and whether NAA levels can recover over time under certain circumstances remain unresolved.

4.1.3. Molecular imaging of glutamate-mediated channels

The decrease in the CBF leads to a marked reduction in ATP with Na^+/K^+ pump failure and an increase in extracellular glutamate which activates glutamate-mediated channels and results in neuronal damage and eventual death.

Glutamate stimulation of α-amino-3-hydroxy-5-methyl-4-isoxazolone-proprionic acid (AMPA) receptors increases sodium uptake by neurons and cellular edema (90). However, glutamatergic stimulation of N-methyl-D-aspartate (NMDA) receptors by glutamate increases intracellular calcium concentrations and cell death (91, 92). NMDA receptors exist as tetrameric subunit assemblies made from both NR1 and NR2 receptor subunits (93-96). The NR2 subunits (NR2A-D) give rise to four receptor subtypes, which have different pharmacological properties and expression patterns in the CNS (97). NR2A and NR2B are the predominant NR2 subunits in the adult forebrain, where stroke most frequently occurs. These subunits have differential roles in supporting neuronal survival and mediating neuronal death and hence have opposing impacts on excitotoxic brain damage after acute brain insults such as stroke and brain trauma. Recently several studies have strongly suggested that it is the NR1/NR2B, not the NR2A-containing, NMDA receptor subpopulation that plays a primary role in triggering intracellular cascades that lead to NMDA- or ischemia-induced neuronal apoptosis and in fact, NR2A is involved in the NMDA-mediated neuronal survival (98-100). Such opposing actions may explain, at least in part, the failure of NMDA receptor antagonism-based clinical trials of stroke and provide a scientific basis for developing novel and effective NMDA receptor-based stroke therapies.

PET tracers targeting the NR2B receptor, by allowing non-invasive imaging in the living brain in stroke models, could facilitate drug discovery and provide new diagnostic tools. Over the last few years several compounds have been synthesized and evaluated as NR2B-selective PET tracers. Despite promising results obtained *in vitro*, all compounds evaluated so far have suffered from low to moderate brain penetration and lack of NR2B-specific binding *in vivo*. Recently, Merck published a new series of NR2B-selective compounds, based on the N-benzyl amidine structure and Arstad *et al.* (97) in a study using three different compounds of N-benzyl amidine class, demonstrated ^{11}C-labelled N-benzyl amidines have a brain uptake suitable for PET imaging. In addition, they were also found to have favorable uptake and retention in the brain, as well as a binding pattern consistent with the expression of the target receptor as measured by *in vitro* autoradiography. However, the metabolism of the compounds tested was too rapid to allow for *in vivo* imaging. Further optimization of this class of compounds may lead to successful PET tracers for the NMDA NR2B subtype receptor (97).

4.1.4. Inflammation and molecular imaging

Local brain inflammation is a pathologic hallmark of ischemic stroke lesions (101, 102) and is spatiotemporally related to the occurrence of delayed apoptotic cell death (103). Phagocyte cells, involving resident microglia and infiltrating macrophages, have both protective and destructive role in stroke. Microglia is activated within minutes of ischemia onset and produces a plethora of inflammatory mediators, which exacerbate tissue damage (104-106), but may also protect the brain against ischemic and excitotoxic injury (107-109). In contrast to the rapid microglia response, blood-derived macrophages are recruited with a delay of at least 24 to 48 hours (110-112). At these later stages, the synthesis of proinflammatory cytokines is already down regulated (113), whereas various anti-inflammatory and protective factors are progressively expressed (114, 115). Thus, inflammatory responses to -brain ischemia are heterogeneous and at cellular level, phagocyte cells represent a potential therapeutic target. To date, most studies on microglia/macrophage response to cerebral ischemia have used cell culture or *ex vivo* histology and several studies in experimental stroke models showed that multimodal MRI comprising diffusion- and perfusion-weighted as well as gadolinium-enhanced imaging is not able to discriminate inflamed from noninflamed infarct subareas (116). Thus, new molecular imaging techniques to monitor phagocytic activity in brain ischemia need to be developed.

Already several years ago, superparamagnetic iron oxide nanoparticles have been introduced as cell-specific contrast agents that can be injected intravenously and are taken up by cells of the mononuclear phagocyte system (117). Based on particle size, one can distinguish superparamagnetic iron oxide (SPIO; ≈60 to 150 nm diameter) from ultrasmall superparamagnetic iron oxide particles (USPIO; ≈20 to 50 nm). SPIO particles are rapidly phagocytosed by cells of the reticuloendothelial system in liver and spleen leading to rapid clearance from the blood pool after intravenous injection. In contrast, circulation times of USPIO are considerably longer which, at least in theory, favors the interaction with phagocyte populations in the blood and lymph nodes. USPIO nanoparticles cause microscopic field gradients that efficiently diphase nearby protons by disrupting the homogeneity of the magnetic field, thereby strongly enhancing the transverse relaxation times T2 and T2* over a length scale much larger than the nanoparticles' size. Hence, they are called T2 contrast agents, and they decrease signal intensity in standard imaging sequences (117). Their relaxivity increases with field strength up to its saturation threshold, with higher MR field strengths producing larger signal intensity changes and hence a higher contrast-to-noise ratio. Accordingly, USPIO agents such as Ferumoxtran-10 (Combidex, Sinerem) are in advanced clinical development for lymph node imaging (118).whereas SPIO particles such as ferumoxide (Endorem, Resovist) have been approved for liver imaging. Despite these differences, both types of contrast agents have been successfully used in the study of inflammatory processes in brain ischemia.(119-124)

In experimental brain ischemia, Rausch *et al.* (119) were the first to use USPIO for macrophage imaging in a model of permanent middle cerebral artery occlusion (pMCAO). In this study, ferumoxtran-10 was injected intravenously into rats at 5 hours after pMCAO followed by repeated MRI on days 1, 2, 4, and 7. On T2-weighted images, patchy areas of signal loss in the infarctions were found until day 4 and decreased thereafter. Essentially similar findings were obtained in a transient ischemia model (120). Using photochemically induced ischemia model, several studies showed accumulation of iron oxide particles in the infarct border zone during subacute stages of lesion development (121, 123, 124). Importantly, iron-related signal changes on MRI were paralleled by macrophage-associated iron deposition detected histochemically on postmortem brain sections. In the study by Kleinschnitz *et al.* (121), SPIO injection between days 5 and 6 after ischemia, but not at earlier time points, caused typical signal loss on T2*-weighted images obtained 24 hours after injection. Thus, based on the assumption that SPIO was primarily taken up by circulating phagocytes, this study suggests that infiltration of SPIO-laden macrophages occurred to a significant extent only at the end of the first week after ischemia. This is in line with earlier results suggesting that the recruitment of hematogenous macrophages likewise occurs in a narrow time interval between days 3 and 6 after ischemia (110-112). Collectively, these findings demonstrate that appropriate timing of contrast agent injection and subsequent MRI is of critical importance for iron oxide particle-based macrophage imaging in brain ischemia.

Microglia and macrophage responses are segregated not only with respect to time, but to some extent also spatially. After focal cortical ischemia, there is secondary involvement of the ipsilateral thalamus attributable to retrograde degeneration of thalamocortical projection fibers (125-127). In these areas of delayed degeneration, strong and long-lasting microglia activation develops, whereas hematogenous macrophages are largely excluded. In the studies reported so far, iron oxide particle-related signal changes were restricted to the primary lesion site and not observed in the thalamus. These observations further support the concept that particle uptake occurs peripherally with subsequent infiltration of iron-laden cells into the lesioned central nervous system parenchyma. Thereby, iron oxide particle-enhanced MRI potentially differs from PET with ^{11}C-PK11195 as a radioactive ligand to peripheral-type benzodiazepine-binding sites on mononuclear phagocytes. Previous studies showed increased binding of ^{11}C-PK11195 in the thalamus ipsilateral to a cortical MCA infarction indicating that ^{11}C-PK11195 PET detects microglia responses in the degenerating areas (126, 127). USPIO uptake and ^{11}C-PK11195 binding may therefore reflect distinct aspects of the cellular inflammatory response to brain ischemia.

Recently Jander *et al.* (122) conducted a trial of USPIO-enhanced MRI in 10 consecutive patients with early ischemic stroke. In their study, USPIO contrast agent was infused 5 to 6 days after stroke onset, which corresponds to the presumed period of hematogenous macrophage recruitment (110, 121) and infarct expansion shown in

quantitative MRI analysis (128, 129). In line with preclinical safety studies (130), USPIO infusions were well tolerated by all patients. To delineate lesion extension, all patients underwent initial stroke MRI, including diffusion- and perfusion-weighted imaging, within 24 hours after stroke. To define the pattern of gadolinium-based contrast medium enhancement, a first follow-up gadolinium-enhanced MRI was performed 4 to 5 days after symptom onset (i.e., 24 hours before USPIO infusion). Two additional scans were obtained at 24 and 48 hours after USPIO infusion. As the main finding, they observed consistent USPIO-related signal changes in all 10 patients, whereas gadolinium enhancement only occurred in three patients. Thus, USPIO enhancement was not a mere epiphenomenon of blood–brain barrier breakdown. Interestingly, their study revealed two distinct components of USPIO-related signal changes, one associated with blood vessels and one representing parenchymal enhancement. Vessel-associated changes appeared as signal loss on T2/T2*-weighted images and decreased from the first to second scan after USPIO infusion, most likely reflecting a transient blood pool effect of the contrast agent. Conversely, parenchymal enhancement was mainly evident on T1-weighted images, increased over time, and matched with the expected distribution of macrophages. They therefore suggest that the increasing USPIO enhancement on T1-weighted images indicates brain infiltration by USPIO-laden macrophages. Similar to these findings, Dousset and colleagues (131) reported prominent signal changes on T1- rather than on T2*-weighted images in patients with multiple sclerosis. The reasons for the distinct USPIO-related signal patterns on T1- versus T2*-weighted images are currently unknown.

These studies raise the perspective that USPIO-enhanced MRI may provide a novel *in vivo* surrogate marker of cellular inflammation in stroke and other central nervous system pathologies. There are a number of open questions that require further study. First of all, the assumption that circulating monocyte-derived phagocytes act as the principal cell type responsible for iron particle uptake after IV injection is so far only based on indirect evidence. Furthermore, even circulating mononuclear phagocytes can be subdivided into subpopulations with distinct phenotypic and functional profiles (132). Thus, USPIO enhancement may reflect the infiltration of a specific macrophage subpopulation, which remains to be identified. Finally, inflammation may not only have deleterious consequences for ischemic lesion progression, but may also mediate beneficial effects such as lesion demarcation, wound healing, and tissue regeneration. So far, the specific functional contribution of macrophages for the development of brain infarction is essentially unknown. USPIO-enhanced MRI may represent an important tool to address this issue both in basic science and clinical studies.

An alternative strategy to image inflammation is to develop MRI contrast agents specifically targeting an inflammatory cellular marker like the endothelial adhesion molecules. E-selectin (CD62E, ELAM-1) is an adhesion molecule expressed on the luminal surface of vascular endothelial cells in inflammation. It serves the function of initiating interactions between the endothelial cell and circulating leukocytes, preceding leukocyte diapedesis into inflamed tissue (133).

Chapman and colleagues showed that anti–E-selectin monoclonal antibodies (MoAbs) labeled with indium-111 or technetium-99m can be used to image activated endothelium *in vivo* in porcine monoarthritis (134-136), as well as inflamed tissues in rheumatoid arthritis (137-139) and inflammatory bowel disease (140). Importantly, radiolabeled anti–E-selectin imaging was much more sensitive than imaging with radiolabeled nonspecific immunoglobulin, demonstrating the advantage of this approach to investigating inflammation over methods that rely on increased endothelial permeability (137).

Exposure to ionizing radiation and the relatively poor anatomic resolution of nuclear gamma cameras limit the value of radiolabeled antibodies in imaging. Therefore, other modalities, including MR imaging (141, 142) and near-infrared optical imaging (143), have been assessed *in vitro* for E-selectin targeting. Furthermore, sialyl Lewis X, a carbohydrate moiety that binds E-selectin, has been conjugated to gadolinium and used to target E-selectin at MR imaging in models of focal brain ischemia (144) and cytokine-mediated inflammation (145). As USPIO nanoparticles degradation occurs through normal physiologic iron-handling pathways (146), it has marked potential safety advantages over gadolinium, which has no known intracellular excretion pathway. Kang *et al.* (141) modified USPIO nanoparticles to bind E-selectin *in vitro* and recently Reynolds *et al.* (147) used an antibody for targeting USPIO, they used $F(ab')_2$ fragments to minimize interactions with Fc receptors or complement. Antibody conjugation of USPIO provides proof-of-principle for the efficacy of targeting E-selectin for *in vivo* MR imaging, allowing a comparison in due course with other, possibly less specific, ligands that bind E-selectin, such as peptides (148, 149) or carbohydrates (144, 145). They showed that antibody-conjugated USPIO can be used for MR imaging of E-selectin expression on vascular endothelium *in vivo*. This could be valuable for diagnosing and monitoring early or occult inflammation and may provide an attractive alternative to established investigations such as those involving radiolabeled leukocytes (150).

4.1.5. Molecular imaging of apoptosis in stroke

Apoptosis, or programmed cell death, has also been suggested as being a contributor to the evolution of the penumbra to necrotic tissue. As protein synthesis is required for apoptosis to occur, it is likely that this mechanism only contributes to the progression of the ischemic lesion in areas of modest ischemia or after reperfusion (151). Therefore, molecular imaging of apoptosis can be a highly useful tool in monitoring of stroke course and its response to treatment.

Imaging of apoptosis in stroke has been attempted with radio-labeled annexin V, a 36 kDa protein that binds to phosphatidylserine (PS), exposed on the cell surface of the apoptotic cell. However, annexin V in stroke imaging was found to underscore the infarct region, while showing multiple bilateral foci of increased signal, extending beyond the regions damaged by the ischemic insult (74, 152, 153). This questionable selectivity and specificity of annexin V for imaging of cell death in stroke may be attributed, at least in part, to its being a relatively large protein, with limited brain access and slow blood clearance. In addition, this probe binds in early apoptosis only on the cell surface, without intracellular uptake and accumulation (154), thus potentially reducing signal/noise ratio.

ApoSense is a novel family of low-molecular weight compounds, designed to address the challenge of apoptosis imaging *in vivo*. It comprises amphipathic compounds that do not cross the plasma membrane of intact viable cells, but perform selective passage through the membrane of apoptotic cells and accumulation in the cytoplasm from the early cellular stages of the death process. Few studies have shown imaging of cell death, both *in vitro* and *in vivo*, by two members of the *ApoSense* family: DDC (*N*,*N*′-didansyl-l-cystine, MW = 707) (155), and NST-732 [(5-dimethylamino)-1-napththalene-sulfonyl-α-ethyl-fluoroalanine, MW = 368) (156). Upon intravenous systemic administration *in vivo* in animal models of disease-related apoptosis, these compounds have been shown to target specifically the cells undergoing cell death, with marked intracellular accumulation.

Reshef *et al.* (157) recently used DDC as a probe for detection of cell death in experimental stroke *in vivo*. DDC manifested selective uptake only by brain areas in the territory of vascular compromise (MCA in this case), and not by other parts of the brain. Within the affected region, uptake was selective only into cells undergoing cell death, with intracellular accumulation of the compound. A sharp border was outlined between intact and cell death regions of the brain. Interestingly, within the same region, conceivably sustaining similar ischemic insult, a mosaic of cells undergoing cell death and intact cells was found, which is characteristic of apoptosis. Detection of cell death by DDC in this study was similar to the pattern of DDC uptake observed in other models of cell death *in vivo*, such as renal injury (155). This study showed the capability of DDC to delineate differential load of cell death in various regions of the infarct. This analysis of the infarct region, according to the differential load of cell death in its various regions, can be useful for accurate and sensitive assessment of the extent of tissue damage and potential reserves of salvageable tissue within the areas suffering from the vascular compromise.

4.1.6. Angiogenesis and molecular imaging

Reperfusion and collateral revascularization of potentially viable tissue is an important factor in determining patient recovery. Angiogenesis within the penumbra begins after the onset of ischemic stroke and the extent of angiogenesis is correlated with a patient's survival time (158) . Although angiogenesis is stimulated by hypoxia, but how the entire process affects outcome after focal cerebral ischemia is still unclear. It has been proposed that angiogenesis resulting from local hypoxia inhibits the degradation of hypoxia-inducible factor-1 (HIF-1), allowing its sustained expression and stimulating expression of vascular endothelial growth factor (VEGF).

Angiogenic growth factors are secreted by infiltrating macrophages, leucocytes and damaged blood platelets, and this probably helps to maintain increased circulatory expression after stroke. Increased VEGF expression was reported in human brain tissue following acute ischemic stroke (159), whilst Issa *et al.* (160) suggested that bFGF (FGF2) upregulation is one of the mechanisms that leads to angiogenesis and neuroprotection in the penumbra region after acute stroke. VEGF, one of the most potent angiogenic factors, is upregulated within hours of stroke and has a strong influence on the growth of new blood vessels after ischemia. Certainly, angiogenesis offers a most promising target for both prevention and amelioration of the devastating consequences of acute ischemic stroke in humans. Furthermore, new studies have suggested that injured vessels, activated vessels, and new vessels produce an array of trophic factors and cytokines, including vascular endothelial growth factor and brain-derived neurotrophic factor, which evoke neurogenesis (161-164) are chemotactic for progenitor cells, and enhance the survival and integration of neuroblasts into the cerebral tissue. These factors also facilitate synaptic activity and plasticity (161) and may have major applications in future cell therapies for stroke.

Although increased expression of growth factors and cytokines occurs in many stroke models, many of the signaling pathways that are responsible for revascularization and neurogenesis have only been subjectively proposed on the basis of *in vitro* studies. Thus, molecular imaging may have a pivotal role in better understanding of these pathophysiological pathways.

VEGF and integrins (particularly αvβ3 integrin) have been identified as favorable targets for imaging angiogenesis, we and others have focused on the development of probes for these specific targets. Although, multimodality imaging of VEGF expression has been reported for many diseases such as cancer, myocardial infarction and ischemia, but *in vivo* imaging of VEGF/VEGFR expression in stroke has been surprisingly understudied.

4.2. Molecular imaging in stroke prevention

Effective stroke prevention is vital to reduce its clinical burden. Accurate carotid imaging is important for effective secondary stroke prevention. There is a need for new adjuncts to risk stratify patients with carotid artery disease as symptomatology and the degree of luminal narrowing, which have been previously used as clinical grounds for surgical intervention, may no longer be appropriate to be solely considered for decision making. Part of the reason for this is that luminal stenosis alone has

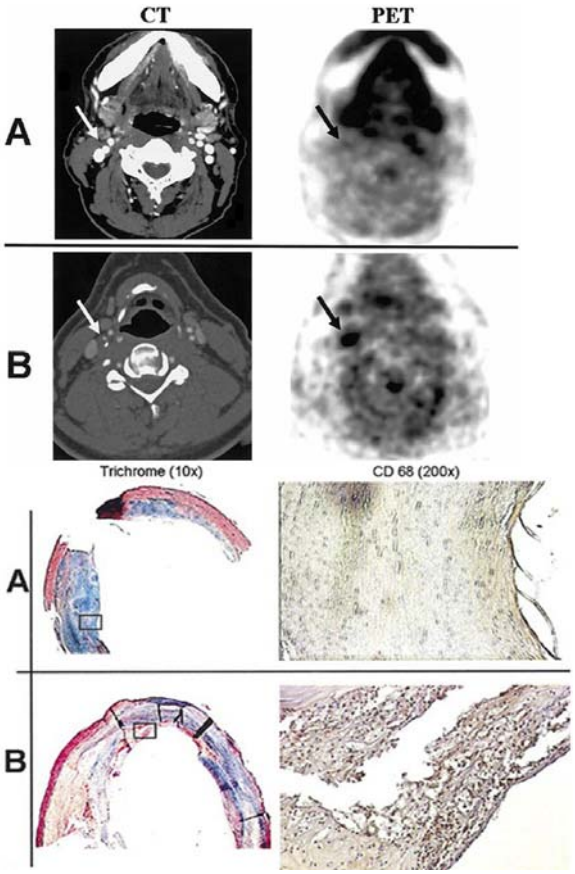

Figure 4. Axial positron emission tomographic (PET) images and the co-registered computed tomographic (CT) images from 2 patients, 1 (patient A) who manifested low 18F-fluorodeoxyglucose (FDG) uptake in the region of the carotid plaque and 1 (patient B) with high FDG uptake in the region of the carotid plaque. The region of the excised carotid plaque is noted with arrows. (A) Carotid plaque specimen taken from the patient with low FDG uptake (patient A). The corresponding trichrome-stained histological specimen demonstrates a collagen-rich plaque with low lipid content, and CD68 staining on the high-powered images demonstrates limited macrophage infiltration. These histological features are consistent with a metabolically stable and potentially clinically stable plaque. (B) Carotid plaque specimen taken from the patient with high FDG uptake (patient B). The corresponding trichrome-stained histological specimen demonstrates a complex plaque with a necrotic core, and the CD68 staining demonstrates intense macrophage infiltration. These histological features are consistent with a metabolically unstable plaque which vulnerable to rupture. Adapted with permission from ref. 174.

been shown not to adequately reflect atheromatous disease burden due to the process of arterial remodeling (165).

The composition and stage of atherosclerotic plaques are clinically more relevant than the severity of stenosis to evaluate the risk of acute ischemic events. The vulnerable carotid atheromatous plaque, considered responsible for many acute ischemic events, usually has a thin fibrous cap, a large lipid pool and macrophage-dense inflammation on or beneath its surface (166). In contrast, stable or "safe" plaque is fibrous, with little lipid and little or no inflammation. Inflammation within atherosclerotic lesions is likely to increase the risk of plaque rupture and subsequent thrombo-embolism (167) and therefore is an obvious target for novel plaque stabilization interventions. Hence there is the need for the development of new imaging techniques for the detection of vulnerable plaques and particularly plaque inflammation.

It has been possible to image carotid plaque inflammation with USPIO enhanced MRI in both animal (168) and *in vivo* human studies (169). The use of a USPIO agent – Sinerem™ (Guerbet, Roissy, France), has allowed the direct visualization of macrophage infiltration of carotid atheroma *in vivo* (169-172). USPIO particles are taken up by activated macrophages in vulnerable plaques and, when clumped in the phagolysosomes produce a strong T_2* susceptibility effect, visible on T_2* weighted sequences as magnetic susceptibility artifacts (MSA) or signal voids.

In addition to the T_2* effect, there is a predominant T_1 shortening effect at low concentrations of USPIO in circulating blood, allowing better visualization of the fibrous cap and suggesting that this contrast agent could be used to detect not only inflammation within vulnerable plaque but also aid in identification of "safer" plaque with a significant fibrous component (171). There are also several studies that have used ^{18}F-fluorodeoxyglucose (^{18}F-FDG) PET imaging for noninvasive measurement of atherosclerotic plaque inflammation (173, 174) (Figure 4).

Biomechanical stress is also considered to be a major determinant of plaque vulnerability (175). Structural analysis has suggested that triggers of plaque rupture include high von Mises stress concentrations on a thin fibrous cap and low vessel wall shear stresses as a result of turbulent blood flow (176, 177). Although physiologically important in a purely biomechanical study, wall shear stress is relatively minor compared with the internal stresses of the plaque (von Mises stresses). Finite element analysis (FEA) techniques has been used successfully to perform stress analysis of vulnerable carotid plaques based on the geometry derived from *in vivo* MRI (178). Li *et al.* (179) showed that the maximal stresses in the symptomatic plaques were higher than those in the asymptomatic ones and they consistently found that the peak stresses within the shoulder regions and thinnest areas of fibrous cap, of the plaque, which seems to support the notion that the location of plaque rupture is associated with the location of the peak stress. Likewise, the authors showed that, in an idealized model of the carotid bifurcation, it is fibrous cap thickness rather than overall luminal stenosis that appears to contribute most to the overall plaque stress.

Recently Tang *et al.* (180) performed a study to investigate whether there is a relationship between the degree of MR-defined inflammation using USPIO and biomechanical stress using FEA, in carotid atheromatous plaques. They have demonstrated that there is a significant relationship between biomechanical stress and USPIO

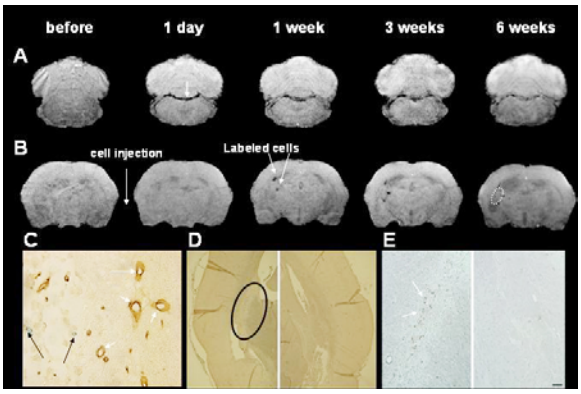

Figure 5. Dynamic migration of transplanted cells in ischemic brain: The dark areas in the 3D MRI were not detected before transplantation of labeled progenitor cells (column Before in A to B). In contrast, the same rat exhibited MRI signals at the cistern at 1 day after injection of superparamagnetic particle labeled cells (A, 1 day, arrow). The dark areas in the 3D MRI first reached the ipsilateral striatum nearby the ipsilateral lateral ventricle within 1 week after transplantation (B, 1 week, arrow). The dark areas in the ipsilateral striatum were clearly visible during the 6 week period. Dark areas were not detected in the contralateral hemisphere at any time points after transplantation (B, 1 day to 6 weeks). Panels A and B represent different levels of coronal sections from the posterior to anterior brain (A, bregma_13.3 mm; B, bregma_1.3 mm). Before and 1 day represent 1 day prior to and 1 day after cell transplantation, and 1 week to 6 weeks indicate weeks after transplantation from a representative rat. Prussian blue staining was used to identify superparamagnetic particle labeled cells on coronal sections. This staining reacts with iron to produce blue color. The Prussian blue staining sections (C) obtained from the same rat 6 weeks after transplantation showed clusters of Prussian blue positive cells indicating superparamagnetic particle labeled cells (see C, black arrows) in the ischemic boundary. These blue cells were localized to angiogenesis areas (C, white arrows). Panels D and E are the vWF immunoreactive images of coronal sections, which matched MRI sections from the same animal sacrificed at 6 weeks, showed an increase in numbers of vWF immunoreactive vessels (left image in D, black line area; left image in the magnified vWF immunostained image E, arrows) in vWF immunostained images. Adapted with permission from ref. 197.

enhanced MR-defined inflammation within carotid atheroma. While there is an obvious association between USPIO and predicted plaque stress from FEA, this of course does not necessarily imply a causative relationship. It remains unclear whether or not the correlation between plaque inflammation and plaque stress is a linear one. This may be difficult to elucidate when there is currently no consensus in the literature as to how best to quantify USPIO uptake in inflammatory carotid atheroma and the relationship between the extent of signal drop seen post-USPIO and macrophage number remains unclear.

Complex biological systems such as atheromatous plaques need to be considered in terms of both their physical mechanical properties and their pathophysiology. The complex interplay between cellular biology and biomechanics is emerging as an extremely important concept for the further understanding of pathological processes and MR imaging will continue to play a major role in uncovering these poorly understood relationships.

4.3. Stem Cell and Stroke Therapy: The role of Molecular Imaging

Stem cells have been used to treat neurological diseases in which neuronal death is the major pathogenetic mechanism, including cerebrovascular and other neurodegenerative diseases (181). Moreover, the first human neural stem cell clinical trial has recently been approved for Batten disease, a pediatric lysosomal storage disease that leads to neuronal loss and death (182). With such advances it becomes important to answer critical questions about the prospects of cell transplantation for stroke therapy.

Stem cells have the capacity to self-renew and differentiate into different cell types, including neurons, astrocytes, and endothelial cells. Stem and progenitor cells are present in fetal cells, immortalized cell lines, umbilical cord blood, bone marrow, and specific organs, including the brain. Animal studies suggest that stem cells (including those from bone marrow) can survive, integrate, and function as neurons in experimental models of stroke (183-186). Because the application of stem cell-based therapies is potentially wide-ranging, specific methods are needed to continuously and noninvasively monitor stem cell survival.

Three-dimensional imaging and *in vivo* cell tracking capabilities allow MRI to provide high-resolution visualization of the fate of cells after transplantation, and the migration of cells after injection (187) (Figure 5). Recently Shyu *et al.* used Gd-DTPA as MRI contrast agent for tracking immortalized human bone marrow stromal cells in stroke treatment in rat. They used Effectene to transfect the MRI contrast agent Gd-DTPA into stem cells, because it is relatively more efficient and less toxic than liposome, calcium phosphate, or viral vectors for transfection into primary cells (188-190).

Many experiments have used other paramagnetic substances to track cell movement under MRI, including iron containing agents (e.g. Feridex) and a new generation of contrast agents magnetodendrimers and particles conjugated with Tat peptides (191). However, magneto dendrimers and particles conjugated with Tat peptides require complicated methods of manufacture. Furthermore, iron-containing agent labeled stem cells transplanted into brain are visualized as signal void images (black signal) using these paramagnetic substances. This can create problems because enlarged “false” black signaling effects of iron-labeled cells can exceed true stem cell mass (191). In addition, iron can be toxic at high concentrations (192), with its accumulation in tissue also catalyzing the Fenton reaction and potentiating oxygen toxicity through the

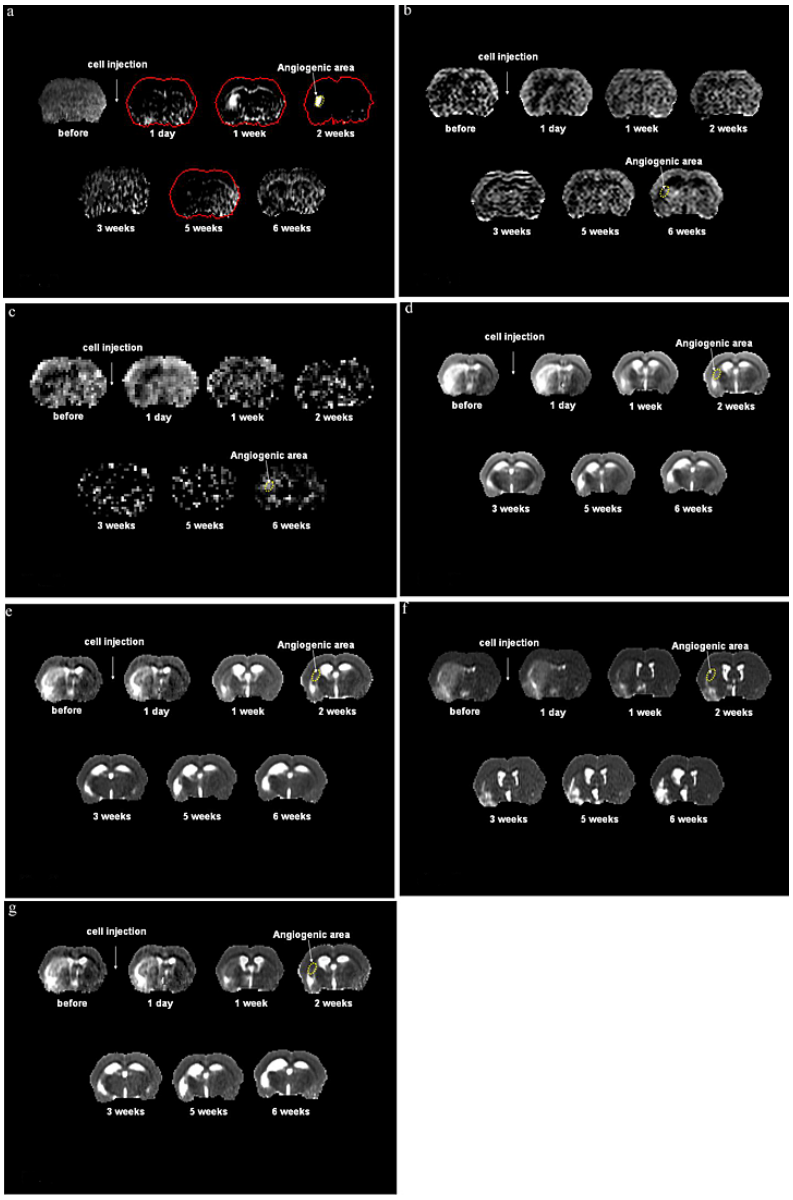

Figure 6. A typical MRI set from a representative animal showing angiogenesis. The temporal evolution of K_i (blood-to-brain transfer constant) (a), CBF (b), CBV (c), T_1 (d), T_{1sat} (T_1 in the presence of an off-resonance irradiation of the macromolecules of brain) (e), T_2 (f), and K_{inv} (the inverse of the apparent forward transfer rate for magnetization transfer) (g) maps, respectively, obtained at various times from 1 day before to 6 weeks after cell transplantation. Adapted with permission from ref. 197.

generation of a wide range of free radical species. Furthermore, leakage of iron or the death of labeled cells may cause the release of iron oxide crystals into tissue, which can result in a potentially toxic uptake in surrounding healthy cells (193). In contrast, the pharmacological properties of Gd-DTPA have been extensively investigated (189) and clinically applied. Under MRI, Gd-DTPA–labeled cells in the brain show increased signal intensity (white signal) rather than void signals. Although the MR detection thresholds in stem cell labeling were lower in the iron-containing particle than that of Gd-DTPA it is highly desirable for clinical applications. In this study cortical neurochemical activity as evaluated by MRS also increased considerably after immortalized human bone marrow stromal cell transplantation.

Cell transplantation therapy for stroke holds great promise. However, many fundamental questions related to the optimal candidate (including the patient age, etiology, anatomic location and size of the infarct, and medical history), the best cell type, the number and concentration of cells, the timing of surgery, the route and site of delivery, and the need for immunosuppression remain to be answered. Furthermore, longer-term studies are required to determine whether the cell-enhanced recovery is sustained and also to determine the tumorigenic potential of the cells.

Clearly, more research is needed to understand the bidirectional interaction between the transplanted cells and the host in which the role of molecular imaging is so important.

5. SUMMARY AND PERSPECTIVE

The development of therapies that will provide substantial beneficial outcome for stroke patients remains in its infancy. As of today, there is only one drug approved by FDA, recombinant tissue plasminogen activator, for the treatment of ischemic stroke. Thus, intense efforts to develop new therapeutics for the disease are inevitable. The great challenge for the development of newer, more effective acute stroke therapies will be to intertwine basic science and clinical trial methodology advances to maximize therapeutic advances for this increasingly common disorder. Translational research that focuses on taking advances in the basic science related to focal brain ischemia and developing therapeutic benefits from them will form the foundation for the future of acute stroke care.

The neuroprotection hypothesis, that agents interfering in the ischemic cascade of cell injury can protect the brain in acute stroke, has faced a setback by the latest news that NXY-059 failed to show benefit in the SAINT II trial (194). The main reasons for its failure was the fact that the site and mechanism of action of NXY-059 were never clearly delineated in an animal model (195, 196), so its mode of action in humans was never understood before moving into the clinic.

A variety of new agents have been shown most recently to improve post-ischemic outcomes in experimental animal models. During the preclinical stage, drug development research relies on animals to evaluate the efficacy of new experimental drugs before clinical trials. Typically since noninvasive preclinical molecular imaging of small animal models of stroke has not been established and is not widely available, experimental studies rely on traditional methods in which animals must be sacrificed for evaluation at each stage of drug development cycle. This leads to unavoidable intersubject variability so that a large number of animals must be sacrificed during the drug development and evaluation process. *In vivo* noninvasive imaging techniques can help reduce the number of animals in the preclinical evaluation of drugs since each animal can serve as its own control, and longitudinal studies are possible.

On the other hand, there is an opportunity to stimulate the brain's own restorative capacity to improve neurological function after stroke. There are both cell-based and pharmaceutical approaches that amplify these restorative reprocesses and lead to improved neurological function in the experimental animal. The brain has the ability to create new neural cells in the adult similar to neurogenesis in the embryo; these neuroblasts express protective proteins and respond to homing signals emerging from the vasculature in the injured tissue. The development of these restorative treatments and the amplification of brain plasticity are also being assisted by the use of Molecular imaging of angiogenesis and the signaling pathways (Figure 6).

Molecular imaging has a pivotal role in identification of effective therapeutic agents not only by providing a better understanding of underlying mechanisms and signaling pathways in neuronal damage following stroke but it can also help us in noninvasive *in vivo* monitoring of the efficacy of these new therapeutic agents.

Additional advances in the time window for successful treatment and maximization of functional deficit reduction can be anticipated with the widespread application of penumbral imaging and the implementation of multimodality treatment paradigms. Molecular imaging techniques are becoming ever more a part of our decision-making and treatment strategies. Refinement of these techniques and the increasing use of multimodal imaging provide not only expected findings that are useful in clinical care of the patient but also provide unexpected findings that have expanded our current knowledge of stroke pathophysiology. The future for developing acute stroke therapies looks increasingly bright.

7. REFERENCE

1. Wang, D.S., M. D. Dake, J. M. Park & M. D. Kuo: Molecular Imaging: a primer for interventionalists and imagers. *Journal of vascular and interventional radiology*, 17, 1405-1423(2006)
2. Tempany, C. M. & B. J. McNeil: Advances in biomedical imaging. *JAMA*, 285, 562-567(2001)
3. Wickline, S. A. & G. M. Lanza: Nanotechnology for molecular imaging and targeted therapy. *Circulation*, 107, 1092-1095 (2003)
4. Phelps, M. E.: Nuclear medicine, molecular imaging, and molecular medicine. *J Nucl Med*, 43, 13N-14N (2002)
5. Thrall, J. H.: How molecular medicine will impact radiology. *Diagnostic imaging*, 19, 23, 27-23, 27(1997)
6. Massoud, T. F. & S. S. Gambhir: Molecular imaging in living subjects: seeing fundamental biological processes in a new light. *Genes Dev*, 17, 545-580 (2003)
7. Kitano, H.: Systems biology: a brief overview. *Science*, 295, 1662-1664 (2002)
8. Serganova, I., M. Doubrovin, J. Vider, V. Ponomarev, S. Soghomonyan, T. Beresten, L. Ageyeva, A. Serganov, S. Cai, J. Balatoni, R. Blasberg & J. Gelovani: Molecular imaging of temporal dynamics and spatial heterogeneity of hypoxia-inducible factor-1 signal transduction activity in tumors in living mice. *Cancer Res*, 64, 6101-6108 (2004)
9. Lindner, J. R.: Assessment of inflammation with contrast ultrasound. *Progress in Cardiovascular Diseases*, 44, 111-120 (2001)
10. Zhao, M., D. A. Beauregard, L. Loizou, B. Davletov & K. M. Brindle: Non-invasive detection of apoptosis using magnetic resonance imaging and a targeted contrast agent. *Nat Med*, 7, 1241-1244 (2001)
11. Schirner, M., A. Menrad, A. Stephens, T. Frenzel, P. Hauff & K. Licha: Molecular imaging of tumor angiogenesis. *Ann N Y Acad Sci*, 1014, 67-75 (2004)

12. Weissleder, R.: Scaling down imaging: molecular mapping of cancer in mice. *Nat Rev Cancer*, 2, 11-18 (2002)
13. Blasberg, R.: Imaging gene expression and endogenous molecular processes: molecular imaging. *J Cereb Blood Flow Metab*, 22, 1157-1164 (2002)
14. Gambhir, S. S., H. R. Herschman, S. R. Cherry, J. R. Barrio, N. Satyamurthy, T. Toyokuni, M. E. Phelps, S. M. Larson, J. Balatoni, R. Finn, M. Sadelain, J. Tjuvajev & R. Blasberg: Imaging transgene expression with radionuclide imaging technologies. *Neoplasia*, 2, 118-138 (2000)
15. Cao, F., S. Lin, X. Xie, P. Ray, M. Patel, X. Zhang, M. Drukker, S. J. Dylla, A. J. Connolly, X. Chen, I. L. Weissman, S. S. Gambhir & J. C. Wu: *In vivo* visualization of embryonic stem cell survival, proliferation, and migration after cardiac delivery. *Circulation*, 113, 1005-1014 (2006)
16. Rudin, M. & R. Weissleder: Molecular imaging in drug discovery and development. *Nat Rev Drug Discov*, 2, 123-131 (2003)
17. Mohammad, Y. M., A. A. Divani, J. F. Kirmani, P. Harris-Lane & A. I. Qureshi: Acute treatment for ischemic stroke in 2004. *Emerg Radiol*, 11, 83-86 (2004)
18. Thom, T., N. Haase, W. Rosamond, V. J. Howard, J. Rumsfeld, T. Manolio, Z. J. Zheng, K. Flegal, C. O'Donnell, S. Kittner, D. Lloyd-Jones, D. C. Goff, Jr., Y. Hong, R. Adams, G. Friday, K. Furie, P. Gorelick, B. Kissela, J. Marler, J. Meigs, V. Roger, S. Sidney, P. Sorlie, J. Steinberger, S. Wasserthiel-Smoller, M. Wilson & P. Wolf: Heart disease and stroke statistics--2006 update: a report from the American Heart Association Statistics Committee and Stroke Statistics Subcommittee. *Circulation*, 113, e85-151 (2006)
19. Rothwell, P. M., A. J. Coull, L. E. Silver, J. F. Fairhead, M. F. Giles, C. E. Lovelock, J. N. E. Redgrave, L. M. Bull, S. J. V. Welch, F. C. Cuthbertson, L. E. Binney, S. A. Gutnikov, P. Anslow, A. P. Banning, D. Mant & Z. Mehta: Population-based study of event-rate, incidence, case fatality, and mortality for all acute vascular events in all arterial territories (Oxford Vascular Study). *Lancet*, 366, 1773-1783 (2005)
20. del Zoppo, G. J., K. Poeck, M. S. Pessin, S. M. Wolpert, A. J. Furlan, A. Ferbert, M. J. Alberts, J. A. Zivin, L. Wechsler & O. Busse: Recombinant tissue plasminogen activator in acute thrombotic and embolic stroke. *Ann Neurol*, 32, 78-86 (1992)
21. Wardlaw, J. M., F. M. Chappell, J. J. K. Best, K. Wartolowska & E. Berry: Non-invasive imaging compared with intra-arterial angiography in the diagnosis of symptomatic carotid stenosis: a meta-analysis. *Lancet*, 367, 1503-1512 (2006)
22. Hacke, W., G. Donnan, C. Fieschi, M. Kaste, R. von Kummer, J. P. Broderick, T. Brott, M. Frankel, J. C. Grotta, E. C. Haley, T. Kwiatkowski, S. R. Levine, C. Lewandowski, M. Lu, P. Lyden, J. R. Marler, S. Patel, B. C. Tilley, G. Albers, E. Bluhmki, M. Wilhelm & S. Hamilton: Association of outcome with early stroke treatment: pooled analysis of ATLANTIS, ECASS, and NINDS rt-PA stroke trials. *Lancet*, 363, 768-774 (2004)
23. Astrup, J., B. K. Siesjö & L. Symon: Thresholds in cerebral ischemia - the ischemic penumbra. *Stroke*, 12, 723-725 (1981)
24. Hakim, A. M.: The cerebral ischemic penumbra. *Can J Neurol Sci*, 14, 557-559 (1987)
25. Kidwell, C. S., J. P. Villablanca & J. L. Saver: Advances in neuroimaging of acute stroke. *Curr Atheroscler Rep*, 2, 126-135 (2000)
26. Heiss, W. D., M. Forsting & H. C. Diener: Imaging in cerebrovascular disease. *Curr Opin Neurol*, 14, 67-75 (2001)
27. Schellinger, P. D., O. Jansen, J. B. Fiebach, O. Pohlers, H. Ryssel, S. Heiland, T. Steiner, W. Hacke & K. Sartor: Feasibility and practicality of MR imaging of stroke in the management of hyperacute cerebral ischemia. *AJNR Am J Neuroradiol*, 21, 1184-1189 (2000)
28. Rosenwasser, R. H. & R. A. Armonda: Diagnostic imaging for stroke. *Clin Neurosurg*, 46, 237-260 (2000)
29. Nakano, S., T. Iseda, H. Kawano, T. Yoneyama, T. Ikeda & S. Wakisaka: Correlation of early CT signs in the deep middle cerebral artery territories with angiographically confirmed site of arterial occlusion. *AJNR Am J Neuroradiol*, 22, 654-659 (2001)
30. Moonis, M. & M. Fisher: Imaging of acute stroke. *Cerebrovasc Dis*, 11, 143-150 (2001)
31. Lee, B. I., H. S. Nam, J. H. Heo & D. I. Kim: Yonsei Stroke Registry. Analysis of 1,000 patients with acute cerebral infarctions. *Cerebrovasc Dis*, 12, 145-151 (2001)
32. Kilpatrick, M. M., H. Yonas, S. Goldstein, A. B. Kassam, J. M. Gebel, L. R. Wechsler, C. A. Jungreis & M. B. Fukui: CT-based assessment of acute stroke: CT, CT angiography, and xenon-enhanced CT cerebral blood flow. *Stroke*, 32, 2543-2549 (2001)
33. Gleason, S., K. L. Furie, M. H. Lev, J. O'Donnell, P. M. McMahon, M. T. Beinfeld, E. Halpern, M. Mullins, G. Harris, W. J. Koroshetz & G. S. Gazelle: Potential influence of acute CT on inpatient costs in patients with ischemic stroke. *Acad Radiol*, 8, 955-964 (2001)
34. Adams, H. P., R. J. Adams, T. Brott, G. J. del Zoppo, A. Furlan, L. B. Goldstein, R. L. Grubb, R. Higashida, C. Kidwell, T. G. Kwiatkowski, J. R. Marler & G. J. Hademenos: Guidelines for the early management of patients with ischemic stroke: A scientific statement from the Stroke Council of the American Stroke Association. *Stroke*, 34, 1056-1083 (2003)
35. Jacobs, L., W. R. Kinkel & R. R. Heffner: Autopsy correlations of computerized tomography: experience with 6,000 CT scans. *Neurology*, 26, 1111-1118 (1976)
36. Chalela, J. A., C. S. Kidwell, L. M. Nentwich, M. Luby, J. A. Butman, A. M. Demchuk, M. D. Hill, N. Patronas, L. Latour & S. Warach: Magnetic resonance imaging and computed tomography in emergency assessment of patients with suspected acute stroke: a prospective comparison. *Lancet*, 369, 293-298 (2007)
37. Warach, S., D. Chien, W. Li, M. Ronthal & R. R. Edelman: Fast magnetic resonance diffusion-weighted imaging of acute human stroke. *Neurology*, 42, 1717-1723 (1992)
38. Warach, S., J. Gaa, B. Siewert, P. Wielopolski & R. R. Edelman: Acute human stroke studied by whole brain echo planar diffusion-weighted magnetic resonance imaging. *Ann Neurol*, 37, 231-241 (1995)
39. Lutsep, H. L., G. W. Albers, A. DeCrespigny, G. N. Kamat, M. P. Marks & M. E. Moseley: Clinical utility of diffusion-weighted magnetic resonance imaging in the

assessment of ischemic stroke. *Ann Neurol*, 41, 574-580 (1997)
40. Barber, P. A., D. G. Darby, P. M. Desmond, Q. Yang, R. P. Gerraty, D. Jolley, G. A. Donnan, B. M. Tress & S. M. Davis: Prediction of stroke outcome with echoplanar perfusion- and diffusion-weighted MRI. *Neurology*, 51, 418-426 (1998)
41. Barber, P. A., D. G. Darby, P. M. Desmond, R. P. Gerraty, Q. Yang, T. Li, D. Jolley, G. A. Donnan, B. M. Tress & S. M. Davis: Identification of major ischemic change. Diffusion-weighted imaging versus computed tomography. *Stroke*, 30, 2059-2065 (1999)
42. Lee, L. J., C. S. Kidwell, J. Alger, S. Starkman & J. L. Saver: Impact on stroke subtype diagnosis of early diffusion-weighted magnetic resonance imaging and magnetic resonance angiography. *Stroke*, 31, 1081-1089 (2000)
43. Lövblad, K. O., H. J. Laubach, A. E. Baird, F. Curtin, G. Schlaug, R. R. Edelman & S. Warach: Clinical experience with diffusion-weighted MR in patients with acute stroke. *AJNR Am J Neuroradiol*, 19, 1061-1066 (1998)
44. Ay, H., F. S. Buonanno, G. Rordorf, P. W. Schaefer, L. H. Schwamm, O. Wu, R. G. Gonzalez, K. Yamada, G. A. Sorensen & W. J. Koroshetz: Normal diffusion-weighted MRI during stroke-like deficits. *Neurology*, 52, 1784-1792 (1999)
45. van Everdingen, K. J., J. van der Grond, L. J. Kappelle, L. M. Ramos & W. P. Mali: Diffusion-weighted magnetic resonance imaging in acute stroke. *Stroke*, 29, 1783-1790 (1998)
46. González, R. G., P. W. Schaefer, F. S. Buonanno, L. H. Schwamm, R. F. Budzik, G. Rordorf, B. Wang, A. G. Sorensen & W. J. Koroshetz: Diffusion-weighted MR imaging: diagnostic accuracy in patients imaged within 6 hours of stroke symptom onset. *Radiology*, 210, 155-162 (1999)
47. Johnson, B. A., J. E. Heiserman, B. P. Drayer & P. J. Keller: Intracranial MR angiography: its role in the integrated approach to brain infarction. *AJNR Am J Neuroradiol*, 15, 901-908 (1994)
48. Dagirmanjian, A., J. S. Ross, N. Obuchowski, J. S. Lewin, J. A. Tkach, P. M. Ruggieri & T. J. Masaryk: High resolution, magnetization transfer saturation, variable flip angle, time-of-flight MRA in the detection of intracranial vascular stenoses. *J Comput Assist Tomogr*, 19, 700-706 (1995)
49. Korogi, Y., M. Takahashi, T. Nakagawa, N. Mabuchi, T. Watabe, Y. Shiokawa, H. Shiga, T. O'Uchi, H. Miki, Y. Horikawa, S. Fujiwara & M. Furuse: Intracranial vascular stenosis and occlusion: MR angiographic findings. *AJNR Am J Neuroradiol*, 18, 135-143 (1997)
50. Wintermark, M., M. Sesay, E. Barbier, K. Borbély, W. P. Dillon, J. D. Eastwood, T. C. Glenn, C. B. Grandin, S. Pedraza, J.-F. Soustiel, T. Nariai, G. Zaharchuk, J.-M. Caillé, V. Dousset & H. Yonas: Comparative overview of brain perfusion imaging techniques. *Stroke*, 36, e83-99 (2005)
51. Eastwood, J. D., M. H. Lev, M. Wintermark, C. Fitzek, D. P. Barboriak, D. M. Delong, T.-Y. Lee, T. Azhari, M. Herzau, V. R. Chilukuri & J. M. Provenzale: Correlation of early dynamic CT perfusion imaging with whole-brain MR diffusion and perfusion imaging in acute hemispheric stroke. *AJNR Am J Neuroradiol*, 24, 1869-1875 (2003)
52. Moustafa, R. R. & J.-C. Baron: Imaging the penumbra in acute stroke. *Curr Atheroscler Rep*, 8, 281-289 (2006)
53. Grolimund, P., R. W. Seiler, R. Aaslid, P. Huber & H. Zurbruegg: Evaluation of cerebrovascular disease by combined extracranial and transcranial Doppler sonography. Experience in 1,039 patients. *Stroke*, 18, 1018-1024 (1987)
54. Camerlingo, M., L. Casto, B. Censori, B. Ferraro, G. C. Gazzaniga & A. Mamoli: Transcranial Doppler in acute ischemic stroke of the middle cerebral artery territories. *Acta Neurol Scand*, 88, 108-111 (1993)
55. Iannuzzi, A., T. Wilcosky, M. Mercuri, P. Rubba, F. A. Bryan & M. G. Bond: Ultrasonographic correlates of carotid atherosclerosis in transient ischemic attack and stroke. *Stroke*, 26, 614-619 (1995)
56. Razumovsky, A. Y., J. H. Gillard, R. N. Bryan, D. F. Hanley & S. M. Oppenheimer: TCD, MRA and MRI in acute cerebral ischemia. *Acta Neurol Scand*, 99, 65-76 (1999)
57. Heiss, W. D.: Best measure of ischemic penumbra: positron emission tomography. *Stroke*, 34, 2534-2535 (2003)
58. Sobesky, J., O. Zaro Weber, F.-G. Lehnhardt, V. Hesselmann, M. Neveling, A. Jacobs & W.-D. Heiss: Does the mismatch match the penumbra? Magnetic resonance imaging and positron emission tomography in early ischemic stroke. *Stroke*, 36, 980-985 (2005)
59. Sobesky, J., O. Zaro Weber, F. G. Lehnhardt, V. Hesselmann, A. Thiel, C. Dohmen, A. Jacobs, M. Neveling & W. D. Heiss: Which time-to-peak threshold best identifies penumbral flow? A comparison of perfusion-weighted magnetic resonance imaging and positron emission tomography in acute ischemic stroke. *Stroke*, 35, 2843-2847 (2004)
60. Jacobs, A. H., A. Winkler, M. G. Castro & P. Lowenstein: Human gene therapy and imaging in neurological diseases. *Eur J Nucl Med Mol Imaging*, 32 Suppl 2, S358-S383 (2005)
61. Baron, J. C.: Perfusion thresholds in human cerebral ischemia: historical perspective and therapeutic implications. *Cerebrovasc Dis*, 11 Suppl 1, 2-8 (2001)
62. Markus, R., D. C. Reutens, S. Kazui, S. Read, P. Wright, B. R. Chambers, J. I. Sachinidis, H. J. Tochon-Danguy & G. A. Donnan: Topography and temporal evolution of hypoxic viable tissue identified by ^{18}F-fluoromisonidazole positron emission tomography in humans after ischemic stroke. *Stroke*, 34, 2646-2652 (2003)
63. Hjort, N., K. Butcher, S. M. Davis, C. S. Kidwell, W. J. Koroshetz, J. Röther, P. D. Schellinger, S. Warach & L. Østergaard: Magnetic resonance imaging criteria for thrombolysis in acute cerebral infarct. *Stroke*, 36, 388-397 (2005)
64. Hjort, N., S. Christensen, C. Sølling, M. Ashkanian, O. Wu, L. Røhl, C. Gyldensted, G. Andersen & L. Østergaard: Ischemic injury detected by diffusion imaging 11 minutes after stroke. *Ann Neurol*, 58, 462-465 (2005)
65. Schramm, P., P. D. Schellinger, E. Klotz, K. Kallenberg, J. B. Fiebach, S. Külkens, S. Heiland, M. Knauth & K. Sartor: Comparison of perfusion computed tomography and computed tomography angiography source

images with perfusion-weighted imaging and diffusion-weighted imaging in patients with acute stroke of less than 6 hours' duration. *Stroke*, 35, 1652-1658 (2004)
66. Lin, W., J.-M. Lee, Y. Z. Lee, K. D. Vo, T. Pilgram & C. Y. Hsu: Temporal relationship between apparent diffusion coefficient and absolute measurements of cerebral blood flow in acute stroke patients. *Stroke*, 34, 64-70 (2003)
67. Hamon, M., R. M. Marié, P. Clochon, O. Coskun, J. M. Constans, F. Viader, P. Courthéoux & J. C. Baron: [Quantitative relationships between ADC and perfusion changes in acute ischemic stroke using combined diffusion-weighted imaging and perfusion MR (DWI/PMR)]. *J Neuroradiol*, 32, 118-124 (2005)
68. Nicoli, F., Y. Lefur, B. Denis, J. P. Ranjeva, S. Confort-Gouny & P. J. Cozzone: Metabolic counterpart of decreased apparent diffusion coefficient during hyperacute ischemic stroke: a brain proton magnetic resonance spectroscopic imaging study. *Stroke*, 34, e82-e87 (2003)
69. Guadagno, J. V., E. A. Warburton, P. S. Jones, T. D. Fryer, D. J. Day, J. H. Gillard, T. A. Carpenter, F. I. Aigbirhio, C. J. Price & J.-C. Baron: The diffusion-weighted lesion in acute stroke: heterogeneous patterns of flow/metabolism uncoupling as assessed by quantitative positron emission tomography. *Cerebrovasc Dis*, 19, 239-246 (2005)
70. Guadagno, J. V., E. A. Warburton, F. I. Aigbirhio, P. Smielewski, T. D. Fryer, S. Harding, C. J. Price, J. H. Gillard, T. A. Carpenter & J.-C. Baron: Does the acute diffusion-weighted imaging lesion represent penumbra as well as core? A combined quantitative PET/MRI voxel-based study. *J Cereb Blood Flow Metab*, 24, 1249-1254 (2004)
71. Loh, P.-S., K. S. Butcher, M. W. Parsons, L. MacGregor, P. M. Desmond, B. M. Tress & S. M. Davis: Apparent diffusion coefficient thresholds do not predict the response to acute stroke thrombolysis. *Stroke*, 36, 2626-2631 (2005)
72. Zhou, J., J. F. Payen, D. A. Wilson, R. J. Traystman & P. C. van Zijl: Using the amide proton signals of intracellular proteins and peptides to detect pH effects in MRI. *Nat Med*, 9, 1085-1090 (2003)
73. Sun, P. Z., J. Zhou, W. Sun, J. Huang & P. C. van Zijl: Detection of the ischemic penumbra using pH-weighted MRI. *J Cereb Blood Flow Metab*, 27, 1129-1136 (2007)
74. Blankenberg, F. G., J. Kalinyak, L. Liu, M. Koike, D. Cheng, M. L. Goris, A. Green, J.-L. Vanderheyden, D. C. Tong & M. A. Yenari: ^{99m}Tc-HYNIC-annexin V SPECT imaging of acute stroke and its response to neuroprotective therapy with anti-Fas ligand antibody. *Eur J Nucl Med Mol Imaging*, 33, 566-574 (2006)
75. Heiss, W.-D., J. Sobesky & V. Hesselmann: Identifying thresholds for penumbra and irreversible tissue damage. *Stroke*, 35, 2671-2674 (2004)
76. Nunn, A., K. Linder & H. W. Strauss: Nitroimidazoles and imaging hypoxia. *Eur J Nucl Med*, 22, 265-280 (1995)
77. Takasawa, M., J. S. Beech, T. D. Fryer, Y. T. Hong, J. L. Hughes, K. Igase, P. S. Jones, R. Smith, F. I. Aigbirhio, D. K. Menon, J. C. Clark & J. C. Baron: Imaging of brain hypoxia in permanent and temporary middle cerebral artery occlusion in the rat using 18F-fluoromisonidazole and positron emission tomography: a pilot study. *J Cereb Blood Flow Metab*, 27, 679-689 (2007)
78. Gadian, D. G., R. S. Frackowiak, H. A. Crockard, E. Proctor, K. Allen, S. R. Williams & R. W. Russell: Acute cerebral ischaemia: concurrent changes in cerebral blood flow, energy metabolites, pH, and lactate measured with hydrogen clearance and ^{31}P and ^{1}H nuclear magnetic resonance spectroscopy. I. Methodology. *J Cereb Blood Flow Metab*, 7, 199-206 (1987)
79. Mullins, M. E.: MR spectroscopy: truly molecular imaging; past, present and future. *Neuroimaging Clin N Am*, 16, 605-18 (2006)
80. Minati, L., M. Grisoli & M. G. Bruzzone: MR spectroscopy, functional MRI, and diffusion-tensor imaging in the aging brain: a conceptual review. *J Geriatr Psychiatry Neurol*, 20, 3-21 (2007)
81. Bruhn, H., J. Frahm, M. L. Gyngell, K. D. Merboldt, W. Hänicke & R. Sauter: Cerebral metabolism in man after acute stroke: new observations using localized proton NMR spectroscopy. *Magn Reson Med*, 9, 126-131 (1989)
82. Duijn, J. H., G. B. Matson, A. A. Maudsley, J. W. Hugg & M. W. Weiner: Human brain infarction: proton MR spectroscopy. *Radiology*, 183, 711-718 (1992)
83. Gideon, P., B. Sperling, P. Arlien-Søborg, T. S. Olsen & O. Henriksen: Long-term follow-up of cerebral infarction patients with proton magnetic resonance spectroscopy. *Stroke*, 25, 967-973 (1994)
84. Mathews, V. P., P. B. Barker, S. J. Blackband, J. C. Chatham & R. N. Bryan: Cerebral metabolites in patients with acute and subacute strokes: concentrations determined by quantitative proton MR spectroscopy. *AJR Am J Roentgenol*, 165, 633-638 (1995)
85. Kimura, T., K. Sako, T. Gotoh, K. Tanaka & T. Tanaka: *In vivo* single-voxel proton MR spectroscopy in brain lesions with ring-like enhancement. *NMR Biomed*, 14, 339-349 (2001)
86. Shimizu, H., T. Kumabe, T. Tominaga, T. Kayama, K. Hara, Y. Ono, K. Sato, N. Arai, S. Fujiwara & T. Yoshimoto: Noninvasive evaluation of malignancy of brain tumors with proton MR spectroscopy. *AJR Am J Roentgenol*, 17, 737-747 (1996)
87. Sappey-Marinier, D., G. Calabrese, H. P. Hetherington, S. N. Fisher, R. Deicken, C. Van Dyke, G. Fein & M. W. Weiner: Proton magnetic resonance spectroscopy of human brain: applications to normal white matter, chronic infarction, and MRI white matter signal hyperintensities. *Magn Reson Med*, 26, 313-327 (1992)
88. Harada, K., O. Honmou, H. Liu, M. Bando, K. Houkin & J. D. Kocsis: Magnetic resonance lactate and lipid signals in rat brain after middle cerebral artery occlusion model. *Brain Res*, 1134, 206-213 (2007)
89. Moffett, J. R., B. Ross, P. Arun, C. N. Madhavarao & A. M. A. Namboodiri: N-Acetylaspartate in the CNS: from neurodiagnostics to neurobiology. *Prog Neurobiol*, 81, 89-131 (2007)
90. Mehta, S. L., N. Manhas & R. Raghubir: Molecular targets in cerebral ischemia for developing novel therapeutics. *Brain Res Rev*, 54, 34-66 (2007)
91. Ientile, R., D. Caccamo, V. Macaione, V. Torre & S. Macaione: NMDA-evoked excitotoxicity increases tissue transglutaminase in cerebellar granule cells. *Neuroscience*, 115, 723-729 (2002)

92. Weinberger, J. M.: Evolving therapeutic approaches to treating acute ischemic stroke. *J Neurol Sci*, 249, 101-109 (2006)
93. Loftis, J. M. & A. Janowsky: The N-methyl-D-aspartate receptor subunit NR2B: localization, functional properties, regulation, and clinical implications. *Pharmacol Ther*, 97, 55-85 (2003)
94. Laurie, D. J., I. Bartke, R. Schoepfer, K. Naujoks & P. H. Seeburg: Regional, developmental and interspecies expression of the four NMDAR2 subunits, examined using monoclonal antibodies. *Mol Brain Res*, 51, 23-32 (1997)
95. Rigby, M., B. Le Bourdellès, R. P. Heavens, S. Kelly, D. Smith, A. Butler, R. Hammans, R. Hills, J. H. Xuereb, R. G. Hill, P. J. Whiting & D. J. Sirinathsinghji: The messenger RNAs for the N-methyl-D-aspartate receptor subunits show region-specific expression of different subunit composition in the human brain. *Neuroscience*, 73, 429-447 (1996)
96. Scherzer, C. R., G. B. Landwehrmeyer, J. A. Kerner, T. J. Counihan, C. M. Kosinski, D. G. Standaert, L. P. Daggett, G. Veliçelebi, J. B. Penney & A. B. Young: Expression of N-methyl-D-aspartate receptor subunit mRNAs in the human brain: hippocampus and cortex. *J Comp Neurol*, 390, 75-90 (1998)
97. Rstad, E., S. Platzer, A. Berthele, L. S. Pilowsky, S. K. Luthra, H.-J. Wester & G. Henriksen: Towards NR2B receptor selective imaging agents for PET-synthesis and evaluation of N-[^{11}C]-(2-methoxy)benzyl (E)-styrene-, 2-naphthyl- and 4-trifluoromethoxyphenylamidine. *Bioorg Med Chem*, 14, 6307-6313 (2006)
98. Zhou, M. & M. Baudry: Developmental changes in NMDA neurotoxicity reflect developmental changes in subunit composition of NMDA receptors. *J Neurosci*, 26, 2956-2963 (2006)
99. DeRidder, M. N., M. J. Simon, R. Siman, Y. P. Auberson, R. Raghupathi & D. F. Meaney: Traumatic mechanical injury to the hippocampus *in vitro* causes regional caspase-3 and calpain activation that is influenced by NMDA receptor subunit composition. *Neurobiol Dis*, 22, 165-176 (2006)
100. Liu, Y., T. P. Wong, M. Aarts, A. Rooyakkers, L. Liu, T. W. Lai, D. C. Wu, J. Lu, M. Tymianski, A. M. Craig & Y. T. Wang: NMDA receptor subunits have differential roles in mediating excitotoxic neuronal death both *in vitro* and *in vivo*. *J Neurosci*, 27, 2846-2857 (2007)
101. Stoll, G., S. Jander & M. Schroeter: Inflammation and glial responses in ischemic brain lesions. *Prog Neurobiol*, 56, 149-171 (1998)
102. del Zoppo, G., I. Ginis, J. M. Hallenbeck, C. Iadecola, X. Wang & G. Z. Feuerstein: Inflammation and stroke: putative role for cytokines, adhesion molecules and iNOS in brain response to ischemia. *Brain Pathol*, 10, 95-112 (2000)
103. Braun, J. S., S. Jander, M. Schroeter, O. W. Witte & G. Stoll: Spatiotemporal relationship of apoptotic cell death to lymphomonocytic infiltration in photochemically induced focal ischemia of the rat cerebral cortex. *Acta Neuropathol*, 92, 255-263 (1996)
104. Banati, R. B., J. Gehrmann, P. Schubert & G. W. Kreutzberg: Cytotoxicity of microglia. *GLIA*, 7, 111-118 (1993)
105. Barone, F. C., B. Arvin, R. F. White, A. Miller, C. L. Webb, R. N. Willette, P. G. Lysko & G. Z. Feuerstein: Tumor necrosis factor-alpha. A mediator of focal ischemic brain injury. *Stroke*, 28, 1233-1244 (1997)
106. Rothwell, N., S. Allan & S. Toulmond: The role of interleukin 1 in acute neurodegeneration and stroke: pathophysiological and therapeutic implications. *J Clin Invest*, 100, 2648-2652 (1997)
107. Mattson, M. P., S. W. Barger, K. Furukawa, A. J. Bruce, T. Wyss-Coray, R. J. Mark & L. Mucke: Cellular signaling roles of TGF beta, TNF alpha and beta APP in brain injury responses and Alzheimer's disease. *Brain Res Rev*, 23, 47-61 (1997)
108. Raivich, G., M. Bohatschek, C. U. Kloss, A. Werner, L. L. Jones & G. W. Kreutzberg: Neuroglial activation repertoire in the injured brain: graded response, molecular mechanisms and cues to physiological function. *Brain Res Rev*, 30, 77-105 (1999)
109. Hallenbeck, J. M.: The many faces of tumor necrosis factor in stroke. *Nat Med*, 8, 1363-1368 (2002)
110. Schroeter, M., S. Jander, I. Huitinga, O. W. Witte & G. Stoll: Phagocytic response in photochemically induced infarction of rat cerebral cortex. The role of resident microglia. *Stroke*, 28, 382-386 (1997)
111. Schilling, M., M. Besselmann, C. Leonhard, M. Mueller, E. B. Ringelstein & R. Kiefer: Microglial activation precedes and predominates over macrophage infiltration in transient focal cerebral ischemia: a study in green fluorescent protein transgenic bone marrow chimeric mice. *Exp Neurol*, 183, 25-33 (2003)
112. Tanaka, R., M. Komine-Kobayashi, H. Mochizuki, M. Yamada, T. Furuya, M. Migita, T. Shimada, Y. Mizuno & T. Urabe: Migration of enhanced green fluorescent protein expressing bone marrow-derived microglia/macrophage into the mouse brain following permanent focal ischemia. *Neuroscience*, 117, 531-539 (2003)
113. Jander, S., M. Schroeter & G. Stoll: Role of NMDA receptor signaling in the regulation of inflammatory gene expression after focal brain ischemia. *J Neuroimmunol*, 109, 181-187 (2000)
114. Wang, X., T. L. Yue, R. F. White, F. C. Barone & G. Z. Feuerstein: Transforming growth factor-beta 1 exhibits delayed gene expression following focal cerebral ischemia. *Brain Res Bull*, 36, 607-609 (1995)
115. Wang, X., C. Louden, T. L. Yue, J. A. Ellison, F. C. Barone, H. A. Solleveld & G. Z. Feuerstein: Delayed expression of osteopontin after focal stroke in the rat. *J Neurosurg Sci*, 18, 2075-2083 (1998)
116. Schroeter, M., C. Franke, G. Stoll & M. Hoehn: Dynamic changes of magnetic resonance imaging abnormalities in relation to inflammation and glial responses after photothrombotic cerebral infarction in the rat brain. *Acta Neuropathol*, 101, 114-122 (2001)
117. Weissleder, R., G. Elizondo, J. Wittenberg, C. A. Rabito, H. H. Bengele & L. Josephson: Ultrasmall superparamagnetic iron oxide: characterization of a new class of contrast agents for MR imaging. *Radiology*, 175, 489-493 (1990)
118. Will, O., S. Purkayastha, C. Chan, T. Athanasiou, A. W. Darzi, W. Gedroyc & P. P. Tekkis: Diagnostic precision of nanoparticle-enhanced MRI for lymph-node metastases: a meta-analysis. *Lancet Oncol*, 7, 52-60 (2006)

119. Rausch, M., A. Sauter, J. Fröhlich, U. Neubacher, E. W. Radü & M. Rudin: Dynamic patterns of USPIO enhancement can be observed in macrophages after ischemic brain damage. *Mag Res Med*, 46, 1018-1022 (2001)
120. Rausch, M., D. Baumann, U. Neubacher & M. Rudin: In-vivo visualization of phagocytotic cells in rat brains after transient ischemia by USPIO. *NMR Biomed*, 15, 278-283 (2002)
121. Kleinschnitz, C., M. Bendszus, M. Frank, L. Solymosi, K. V. Toyka & G. Stoll: *In vivo* monitoring of macrophage infiltration in experimental ischemic brain lesions by magnetic resonance imaging. *J Cereb Blood Flow Metab*, 23, 1356-1361 (2003)
122. Saleh, A., M. Schroeter, C. Jonkmanns, H.-P. Hartung, U. Mödder & S. Jander: *In vivo* MRI of brain inflammation in human ischaemic stroke. *Brain*, 127, 1670-1677 (2004)
123. Saleh, A., D. Wiedermann, M. Schroeter, C. Jonkmanns, S. Jander & M. Hoehn: Central nervous system inflammatory response after cerebral infarction as detected by magnetic resonance imaging. *NMR Biomed*, 17, 163-169 (2004)
124. Schroeter, M., A. Saleh, D. Wiedermann, M. Hoehn & S. Jander: Histochemical detection of ultrasmall superparamagnetic iron oxide (USPIO) contrast medium uptake in experimental brain ischemia. *Mag Res Med*, 52, 403-406 (2004)
125. Myers, R., L. G. Manjil, R. S. Frackowiak & J. E. Cremer: [^{3}H]PK 11195 and the localisation of secondary thalamic lesions following focal ischaemia in rat motor cortex. *Neurosci Lett*, 133, 20-24 (1991)
126. Pappata, S., M. Levasseur, R. N. Gunn, R. Myers, C. Crouzel, A. Syrota, T. Jones, G. W. Kreutzberg & R. B. Banati: Thalamic microglial activation in ischemic stroke detected *in vivo* by PET and [^{11}C]PK1195. *Neurology*, 55, 1052-1054 (2000)
127. Schroeter, M., P. Zickler, D. T. Denhardt, H.-P. Hartung & S. Jander: Increased thalamic neurodegeneration following ischaemic cortical stroke in osteopontin-deficient mice. *Brain*, 129, 1426-1437 (2006)
128. Beaulieu, C., A. de Crespigny, D. C. Tong, M. E. Moseley, G. W. Albers & M. P. Marks: Longitudinal magnetic resonance imaging study of perfusion and diffusion in stroke: evolution of lesion volume and correlation with clinical outcome. *Ann Neurol*, 46, 568-578 (1999)
129. Ritzl, A., S. Meisel, H.-J. Wittsack, G. R. Fink, M. Siebler, U. Mödder & R. J. Seitz: Development of brain infarct volume as assessed by magnetic resonance imaging (MRI): follow-up of diffusion-weighted MRI lesions. *J Mag Res Imaging*, 20, 201-207 (2004)
130. Doerfler, A., T. Engelhorn, S. Heiland, M. Knauth, I. Wanke & M. Forsting: MR contrast agents in acute experimental cerebral ischemia: potential adverse impacts on neurologic outcome and infarction size. *J Mag Res Imaging*, 11, 418-424 (2000)
131. Dousset, V., B. Brochet, M. S. A. Deloire, L. Lagoarde, B. Barroso, J. M. Caille & K. G. Petry: MR imaging of relapsing multiple sclerosis patients using ultra-small-particle iron oxide and compared with gadolinium. *AJNR Am J Neuroradiol*, 27, 1000-1005 (2006)
132. Geissmann, F., S. Jung & D. R. Littman: Blood monocytes consist of two principal subsets with distinct migratory properties. *Immunity*, 19, 71-82 (2003)
133. Kansas, G. S.: Selectins and their ligands: current concepts and controversies. *Blood*, 88, 3259-3287 (1996)
134. Chapman, P. T., F. Jamar, A. A. Harrison, R. M. Binns, A. M. Peters & D. O. Haskard: Noninvasive imaging of E-selectin expression by activated endothelium in urate crystal-induced arthritis. *Arthritis Rheum*, 37, 1752-1756 (1994)
135. Keelan, E. T., A. A. Harrison, P. T. Chapman, R. M. Binns, A. M. Peters & D. O. Haskard: Imaging vascular endothelial activation: an approach using radiolabeled monoclonal antibodies against the endothelial cell adhesion molecule E-selectin. *J Nucl Med*, 35, 276-281 (1994)
136. Jamar, F., P. T. Chapman, A. A. Harrison, R. M. Binns, D. O. Haskard & A. M. Peters: Inflammatory arthritis: imaging of endothelial cell activation with an indium-111-labeled F(ab')2 fragment of anti-E-selectin monoclonal antibody. *Radiology*, 194, 843-850 (1995)
137. Chapman, P. T., F. Jamar, E. T. Keelan, A. M. Peters & D. O. Haskard: Use of a radiolabeled monoclonal antibody against E-selectin for imaging of endothelial activation in rheumatoid arthritis. *Arthritis Rheum*, 39, 1371-1375 (1996)
138. Jamar, F., P. T. Chapman, D. H. Manicourt, D. M. Glass, D. O. Haskard & A. M. Peters: A comparison between ^{111}In-anti-E-selectin mAb and ^{99m}Tc-labelled human non-specific immunoglobulin in radionuclide imaging of rheumatoid arthritis. *Br J Radiol*, 70, 473-481 (1997)
139. Jamar, F., F. A. Houssiau, J. P. Devogelaer, P. T. Chapman, D. O. Haskard, V. Beaujean, C. Beckers, D. H. Manicourt & A. M. Peters: Scintigraphy using a technetium ^{99m}Tc-labelled anti-E-selectin Fab fragment in rheumatoid arthritis. *Rheumatology*, 41, 53-61 (2002)
140. Bhatti, M., P. Chapman, M. Peters, D. Haskard & H. J. Hodgson: Visualising E-selectin in the detection and evaluation of inflammatory bowel disease. *Gut*, 43, 40-47(1998)
141. Kang, H. W., L. Josephson, A. Petrovsky, R. Weissleder & A. Bogdanov: Magnetic resonance imaging of inducible E-selectin expression in human endothelial cell culture. *Bioconjug Chem*, 13, 122-127 (2002)
142. Mulder, W. J. M., G. J. Strijkers, A. W. Griffioen, L. van Bloois, G. Molema, G. Storm, G. A. Koning & K. Nicolay: A liposomal system for contrast-enhanced magnetic resonance imaging of molecular targets. *Bioconjug Chem*, 15, 799-806 (2004)
143. Kang, H. W., R. Weissleder & A. Bogdanov: Targeting of MPEG-protected polyamino acid carrier to human E-selectin *in vitro*. *Amino Acids*, 23, 301-308 (2002)
144. Barber, P. A., T. Foniok, D. Kirk, A. M. Buchan, S. Laurent, S. Boutry, R. N. Muller, L. Hoyte, B. Tomanek & U. I. Tuor: MR molecular imaging of early endothelial activation in focal ischemia. *Ann Neurol*, 56, 116-120 (2004)
145. Sibson, N. R., A. M. Blamire, M. Bernades-Silva, S. Laurent, S. Boutry, R. N. Muller, P. Styles & D. C. Anthony: MRI detection of early endothelial activation in brain inflammation. *Mag Res Med*, 51, 248-252 (2004)

146. Petersein, J., S. Saini & R. Weissleder: Liver. II: Iron oxide-based reticuloendothelial contrast agents for MR imaging. Clinical review. *Magn Reson Imaging Clin N Am*, 4, 53-60 (1996)
147. Reynolds, P. R., D. J. Larkman, D. O. Haskard, J. V. Hajnal, N. L. Kennea, A. J. T. George & A. D. Edwards: Detection of vascular expression of E-selectin *in vivo* with MR imaging. *Radiology*, 241, 469-476 (2006)
148. Zinn, K. R., T. R. Chaudhuri, C. A. Smyth, Q. Wu, H. G. Liu, M. Fleck, J. D. Mountz & J. M. Mountz: Specific targeting of activated endothelium in rat adjuvant arthritis with a ^{99m}Tc-radiolabeled E-selectin-binding peptide. *Arthritis Rheum*, 42, 641-649 (1999)
149. Gratz, S., M. Béhé, O. C. Boerman, E. Kunze, H. Schulz, H. Eiffert, T. O'Reilly, T. M. Behr, C. Angerstein, K. Nebendahl, F. Kauer & W. Becker: ^{99m}Tc-E-selectin binding peptide for imaging acute osteomyelitis in a novel rat model. *Nucl Med Comm*, 22, 1003-1013 (2001)
150. Peters, A. M.: Imaging inflammation: current role of labeled autologous leukocytes. *J Nucl Med*, 33, 65-67 (1992)
151. Fisher, M.: Characterizing the target of acute stroke therapy. *Stroke*, 28, 866-872 (1997)
152. Lorberboym, M., F. G. Blankenberg, M. Sadeh & Y. Lampl: *In vivo* imaging of apoptosis in patients with acute stroke: correlation with blood-brain barrier permeability. *Brain Res*, 1103, 13-19 (2006)
153. Mari, C., M. Karabiyikoglu, M. L. Goris, J. F. Tait, M. A. Yenari & F. G. Blankenberg: Detection of focal hypoxic-ischemic injury and neuronal stress in a rodent model of unilateral MCA occlusion/reperfusion using radiolabeled annexin V. *Eur J Nucl Med Mol Imaging*, 31, 733-739 (2004)
154. Boersma, H. H., B. L. J. H. Kietselaer, L. M. L. Stolk, A. Bennaghmouch, L. Hofstra, J. Narula, G. A. K. Heidendal & C. P. M. Reutelingsperger: Past, present, and future of annexin A5: from protein discovery to clinical applications. *J Nucl Med*, 46, 2035-2050 (2005)
155. Damianovich, M., I. Ziv, S. N. Heyman, S. Rosen, A. Shina, D. Kidron, T. Aloya, H. Grimberg, G. Levin, A. Reshef, A. Bentolila, A. Cohen & A. Shirvan: ApoSense: a novel technology for functional molecular imaging of cell death in models of acute renal tubular necrosis. *Eur J Nucl Med Mol Imaging*, 33, 281-291 (2006)
156. Aloya, R., A. Shirvan, H. Grimberg, A. Reshef, G. Levin, D. Kidron, A. Cohen & I. Ziv: Molecular imaging of cell death *in vivo* by a novel small molecule probe. *Apoptosis*, 11, 2089-2101(2006)
157. Reshef, A., A. Shirvan, H. Grimberg, G. Levin, A. Cohen, A. Mayk, D. Kidron, R. Djaldetti, E. Melamed & I. Ziv: Novel molecular imaging of cell death in experimental cerebral stroke. *Brain Res*, 1144, 156-164 (2007)
158. Krupinski, J., J. Kaluza, P. Kumar, S. Kumar & J. M. Wang: Role of angiogenesis in patients with cerebral ischemic stroke. *Stroke*, 25, 1794-1798 (1994)
159. Issa, R., J. Krupinski, T. Bujny, S. Kumar, J. Kaluza & P. Kumar: Vascular endothelial growth factor and its receptor, KDR, in human brain tissue after ischemic stroke. *Lab Invest*, 79, 417-425 (1999)
160. Issa, R., A. AlQteishat, N. Mitsios, M. Saka, J. Krupinski, E. Tarkowski, J. Gaffney, M. Slevin, S. Kumar & P. Kumar: Expression of basic fibroblast growth factor mRNA and protein in the human brain following ischaemic stroke. *Angiogenesis*, 8, 53-62 (2005)
161. Chen, J., Z. G. Zhang, Y. Li, Y. Wang, L. Wang, H. Jiang, C. Zhang, M. Lu, M. Katakowski, C. S. Feldkamp & M. Chopp: Statins induce angiogenesis, neurogenesis, and synaptogenesis after stroke. *Ann Neurol*, 53, 743-751 (2003)
162. Leventhal, C., S. Rafii, D. Rafii, A. Shahar & S. A. Goldman: Endothelial trophic support of neuronal production and recruitment from the adult mammalian subependyma. *Mol Cell Neurosci*, 13, 450-464 (1999)
163. Louissaint, A., Jr., S. Rao, C. Leventhal & S. A. Goldman: Coordinated interaction of neurogenesis and angiogenesis in the adult songbird brain. *Neuron*, 34, 945-960 (2002)
164. Meng, H., Z. Zhang, R. Zhang, X. Liu, L. Wang, A. M. Robin & M. Chopp: Biphasic effects of exogenous VEGF on VEGF expression of adult neural progenitors. *Neurosci Lett*, 393, 97-101 (2006)
165. Pasterkamp, G. & P. C. Smits: Imaging of atherosclerosis. Remodelling of coronary arteries. *J Cardiovasc Risk*, 9, 229-235 (2002)
166. Naghavi, M., P. Libby, E. Falk, S. W. Casscells, S. Litovsky, J. Rumberger, J. J. Badimon, C. Stefanadis, P. Moreno, G. Pasterkamp, Z. Fayad, P. H. Stone, S. Waxman, P. Raggi, M. Madjid, A. Zarrabi, A. Burke, C. Yuan, P. J. Fitzgerald, D. S. Siscovick, C. L. de Korte, M. Aikawa, K. E. Juhani Airaksinen, G. Assmann, C. R. Becker, J. H. Chesebro, A. Farb, Z. S. Galis, C. Jackson, I.-K. Jang, W. Koenig, R. A. Lodder, K. March, J. Demirovic, M. Navab, S. G. Priori, M. D. Rekhter, R. Bahr, S. M. Grundy, R. Mehran, A. Colombo, E. Boerwinkle, C. Ballantyne, W. Insull, R. S. Schwartz, R. Vogel, P. W. Serruys, G. K. Hansson, D. P. Faxon, S. Kaul, H. Drexler, P. Greenland, J. E. Muller, R. Virmani, P. M. Ridker, D. P. Zipes, P. K. Shah & J. T. Willerson: From vulnerable plaque to vulnerable patient: a call for new definitions and risk assessment strategies: Part I. *Circulation*, 108, 1664-1672 (2003)
167. Nighoghossian, N., L. Derex & P. Douek: The vulnerable carotid artery plaque: current imaging methods and new perspectives. *Stroke*, 36, 2764-2772 (2005)
168. Ruehm, S. G., C. Corot, P. Vogt, S. Kolb & J. F. Debatin: Magnetic resonance imaging of atherosclerotic plaque with ultrasmall superparamagnetic particles of iron oxide in hyperlipidemic rabbits. *Circulation*, 103, 415-422 (2001)
169. Trivedi, R. A., C. Mallawarachi, J.-M. U-King-Im, M. J. Graves, J. Horsley, M. J. Goddard, A. Brown, L. Wang, P. J. Kirkpatrick, J. Brown & J. H. Gillard: Identifying inflamed carotid plaques using *in vivo* USPIO-enhanced MR imaging to label plaque macrophages. *Arterioscler Thromb Vasc Biol*, 26, 1601-1606 (2006)
170. Trivedi, R. A., J.-M. U-King-Im, M. J. Graves, J. J. Cross, J. Horsley, M. J. Goddard, J. N. Skepper, G. Quartey, E. Warburton, I. Joubert, L. Wang, P. J. Kirkpatrick, J. Brown & J. H. Gillard: *In vivo* detection of macrophages in human carotid atheroma: temporal dependence of ultrasmall superparamagnetic particles of iron oxide-enhanced MRI. *Stroke*, 35, 1631-1635 (2004)
171. Tang, T., S. P. S. Howarth, S. R. Miller, R. Trivedi, M. J. Graves, J. U. King-Im, Z. Y. Li, A. P. Brown, P. J.

Kirkpatrick, M. E. Gaunt & J. H. Gillard: Assessment of inflammatory burden contralateral to the symptomatic carotid stenosis using high-resolution ultrasmall, superparamagnetic iron oxide-enhanced MRI. *Stroke*, 37, 2266-2270 (2006)
172. Trivedi, R. A., J. M. U-King-Im, M. J. Graves, P. J. Kirkpatrick & J. H. Gillard: Noninvasive imaging of carotid plaque inflammation. *Neurology*, 63, 187-188 (2004)
173. Tawakol, A., R. Q. Migrino, U. Hoffmann, S. Abbara, S. Houser, H. Gewirtz, J. E. Muller, T. J. Brady & A. J. Fischman: Noninvasive *in vivo* measurement of vascular inflammation with F-18 fluorodeoxyglucose positron emission tomography. *J Nucl Cardiol*, 12, 294-301 (2005)
174. Tawakol, A., R. Q. Migrino, G. G. Bashian, S. Bedri, D. Vermylen, R. C. Cury, D. Yates, G. M. LaMuraglia, K. Furie, S. Houser, H. Gewirtz, J. E. Muller, T. J. Brady & A. J. Fischman: *In vivo* 18F-fluorodeoxyglucose positron emission tomography imaging provides a noninvasive measure of carotid plaque inflammation in patients. *J Am Coll Cardiol*, 48, 1818-1824 (2006)
175. Richardson, P. D.: Biomechanics of plaque rupture: progress, problems, and new frontiers. *Ann Biomed Eng*, 30, 524-536 (2002)
176. Loree, H. M., R. D. Kamm, R. G. Stringfellow & R. T. Lee: Effects of fibrous cap thickness on peak circumferential stress in model atherosclerotic vessels. *Circulation Res*, 71, 850-858 (1992)
177. Richardson, P. D., M. J. Davies & G. V. Born: Influence of plaque configuration and stress distribution on fissuring of coronary atherosclerotic plaques. *Lancet*, 2, 941-944 (1989)
178. Li, Z.-Y., S. Howarth, R. A. Trivedi, J. M. U-King-Im, M. J. Graves, A. Brown, L. Wang & J. H. Gillard: Stress analysis of carotid plaque rupture based on *in vivo* high resolution MRI. *J Biomech*, 39, 2611-2622 (2006)
179. Li, Z.-Y., S. P. S. Howarth, T. Tang & J. H. Gillard: How critical is fibrous cap thickness to carotid plaque stability? A flow-plaque interaction model. *Stroke*, 37, 1195-1199 (2006)
180. Tang, T. Y., S. P. Howarth, Z. Y. Li, S. R. Miller, M. J. Graves, J. M. U-King-Im, R. A. Trivedi, S. R. Walsh, A. P. Brown, P. J. Kirkpatrick, M. E. Gaunt & J. H. Gillard: Correlation of carotid atheromatous plaque inflammation with biomechanical stress: Utility of USPIO enhanced MR imaging and finite element analysis. *Atherosclerosis* (2007) Mar 8; [Epub ahead of print]
181. Li, Y., J. Chen, X. G. Chen, L. Wang, S. C. Gautam, Y. X. Xu, M. Katakowski, L. J. Zhang, M. Lu, N. Janakiraman & M. Chopp: Human marrow stromal cell therapy for stroke in rat: neurotrophins and functional recovery. *Neurology*, 59, 514-523 (2002)
182. Taupin, P.: HuCNS-SC (StemCells). *Curr Opin Mol Ther*, 8, 156-163 (2006)
183. Mezey, E., K. J. Chandross, G. Harta, R. A. Maki & S. R. McKercher: Turning blood into brain: cells bearing neuronal antigens generated *in vivo* from bone marrow. *Science*, 290, 1779-1782 (2000)
184. Brazelton, T. R., F. M. Rossi, G. I. Keshet & H. M. Blau: From marrow to brain: expression of neuronal phenotypes in adult mice. *Science*, 290, 1775-1779 (2000)
185. Chen, J., Y. Li, L. Wang, Z. Zhang, D. Lu, M. Lu & M. Chopp: Therapeutic benefit of intravenous administration of bone marrow stromal cells after cerebral ischemia in rats. *Stroke*, 32, 1005-1011 (2001)
186. Shen, L. H., Y. Li, J. Chen, A. Zacharek, Q. Gao, A. Kapke, M. Lu, K. Raginski, P. Vanguri, A. Smith & M. Chopp: Therapeutic benefit of bone marrow stromal cells administered 1 month after stroke. *J Cereb Blood Flow Metab*, 27, 6-13 (2007)
187. Smith, B. R., G. A. Johnson, E. V. Groman & E. Linney: Magnetic resonance microscopy of mouse embryos. *Proc Natl Acad Sci U S A*, 91, 3530-3533 (1994)
188. van den Bos, E. J., A. Wagner, H. Mahrholdt, R. B. Thompson, Y. Morimoto, B. S. Sutton, R. M. Judd & D. A. Taylor: Improved efficacy of stem cell labeling for magnetic resonance imaging studies by the use of cationic liposomes. *Cell Transplant*, 12, 743-756 (2003)
189. Daldrup-Link, H. E., M. Rudelius, R. A. J. Oostendorp, M. Settles, G. Piontek, S. Metz, H. Rosenbrock, U. Keller, U. Heinzmann, E. J. Rummeny, J. Schlegel & T. M. Link: Targeting of hematopoietic progenitor cells with MR contrast agents. *Radiology*, 228, 760-767 (2003)
190. Endesfelder, S., S. Bucher, A. Kliche, R. Reszka & A. Speer: Transfection of normal primary human skeletal myoblasts with p21 and p57 antisense oligonucleotides to improve their proliferation: a first step towards an alternative molecular therapy approach of Duchenne muscular dystrophy. *J Mol Med*, 81, 355-362 (2003)
1911. Bulte, J. W., T. Douglas, B. Witwer, S. C. Zhang, E. Strable, B. K. Lewis, H. Zywicke, B. Miller, P. van Gelderen, B. M. Moskowitz, I. D. Duncan & J. A. Frank: Magnetodendrimers allow endosomal magnetic labeling and *in vivo* tracking of stem cells. *Nat Biotechnol*, 19, 1141-1147 (2001)
192. Crichton, R. R., S. Wilmet, R. Legssyer & R. J. Ward: Molecular and cellular mechanisms of iron homeostasis and toxicity in mammalian cells. *J Inorg Biochem*, 91, 9-18 (2002)
193. Qian, S. Y. & G. R. Buettner: Iron and dioxygen chemistry is an important route to initiation of biological free radical oxidations: an electron paramagnetic resonance spin trapping study. *Free Radic Biol Med*, 26, 1447-1456 (1999)
194. Hill, M. D.: Stroke: the dashed hopes of neuroprotection. *Lancet Neurol*, 6, 2-3 (2007)
195. Marshall, J. W., A. R. Green & R. M. Ridley: Comparison of the neuroprotective effect of clomethiazole, AR-R15896AR and NXY-059 in a primate model of stroke using histological and behavioural measures. *Brain Res*, 972, 119-126 (2003)
196. Buchan, A. M. & J. Kennedy: Strategies for therapy in acute ischemic stroke. *Nat Clin Pract Neurol*, 3, 2-3 (2007)
197. Jiang, Q., Z. G. Zhang, G. L. Ding, L. Zhang, J. R. Ewing, L. Wang, R. Zhang, L. Li, M. Lu, H. Meng, A. S. Arbab, J. Hu, Q. J. Li, D. S. Pourabdollah Nejad, H. Athiraman & M. Chopp: Investigation of neural progenitor cell induced angiogenesis after embolic stroke in rat using MRI. *Neuroimage*, 28, 698-707 (2005)

Abbreviations: SPECT: single photon emission computed tomography; PET: positron emission tomography; CT:

computed tomography; MRI: magnetic resonance imaging; US: ultrasound; tPA: tissue plasminogen activator; DWI: Diffusion-weighted imaging; ADC: apparent diffusion coefficient; PWI: perfusion-weighted imaging; MRA: magnetic resonance angiography; DSA: digital subtraction angiography; CDUS: Carotid Duplex ultrasound; TCD: transcranial Doppler; CBF: cerebral blood flow; CBV: cerebral blood volume; TTP: time to peak; MTT: mean transit time; CMRO2: metabolic rate of oxygen consumption; OEF: rate of oxygen extraction; ^{18}F-FMISO: ^{18}F-fluoromisonidazole; MCAO: middle cerebral artery occlusion; NAA: *n* -acetyl aspartate; ppm: parts per million; AHA: American Heart Association; TE: echo time; MRS: MR spectroscopy; STEAM: stimulated echo acquisition mode; SNR: signal to noise ratio; AMPA: α-amino-3-hydroxy-5-methyl-4-isoxazolone-proprionic acid; NMDA: N-methyl-D-aspartate; SPIO: superparamagnetic iron oxide; MoAbs: monoclonal antibodies; USPIO: ultrasmall superparamagnetic iron oxide particles; PS: phosphatidylserine; DDC: *N*,*N*′-didansyl-L-cystine; HIF-1: hypoxia-inducible factor-1; VEGF: vascular endothelial growth factor; MSA: magnetic susceptibility artifacts; FEA: Finite element analysis; 1H-MRS: proton magnetic resonance spectroscopy.

Key Words: Molecular Imaging, Stroke, Inflammation, Apoptosis, Angiogenesis, Stem cell therapy, Review

Send correspondence to: Xiaoyuan Chen, PhD, the Molecular Imaging Program at Stanford (MIPS), Department of Radiology and Bio-X Program, Stanford University School of Medicine, 1201 Welch Rd, P095, Stanford, CA 94305, Tel: 650-725-0950, Fax: 650-736-7925, E-mail: shawchen@stanford.edu

http://www.bioscience.org/current/vol13.htm